Article

Cell Reports

# The Phosphatase Dusp7 Drives Meiotic Resumption and Chromosome Alignment in Mouse Oocytes

## Graphical Abstract

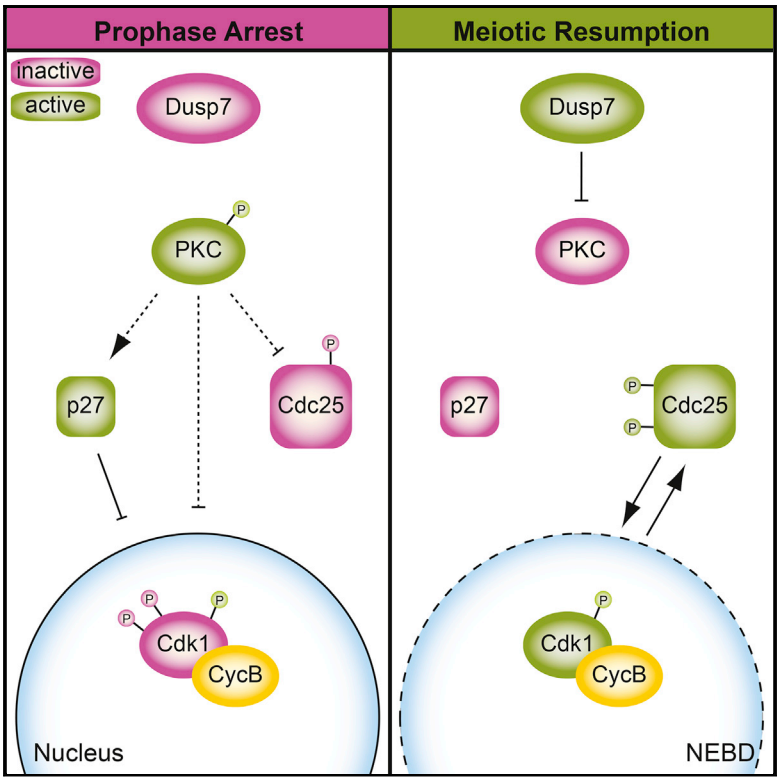


## Authors

Thomas Tischer, Melina Schuh

## Correspondence

melina.schuh@mpibpc.mpg.de

## In Brief

Tischer and Schuh study how oocytes resume meiosis after a prolonged prophase arrest. They show that the phosphatase DUSP7 drives meiotic resumption by dephosphorylating and inactivating conventional protein kinase C (cPKC) isoforms. Hyperactivation of cPKC isoforms in the absence of DUSP7 causes a decrease in the activity of the cell-cycle-regulating kinase Cdk1/Cyclin B, preventing meiotic resumption.

## Highlights

- The phosphatase DUSP7 is an essential regulator of meiotic resumption
- DUSP7 dephosphorylates and inactivates cPKC isoforms
- Inactivation of cPKC isoforms is essential for the timely activation of Cdk1/CycB

Tischer & Schuh, 2016, Cell Reports *17*, 1426–1437
October 25, 2016 © 2016 The Authors.
http://dx.doi.org/10.1016/j.celrep.2016.10.007

CellPress

OPEN ACCESS
CellPress

Cell Reports
Article

# The Phosphatase Dusp7 Drives Meiotic Resumption and Chromosome Alignment in Mouse Oocytes

Thomas Tischer[1] and Melina Schuh[1,2,3,*]
[1]Medical Research Council, Laboratory of Molecular Biology, Cambridge Biomedical Campus, Francis Crick Ave., Cambridge CB2 0QH, UK
[2]Max Planck Institut for Biophysical Chemistry, Am Faßberg 11, 37077 Göttingen, Germany
[3]Lead Contact
*Correspondence: melina.schuh@mpibpc.mpg.de
http://dx.doi.org/10.1016/j.celrep.2016.10.007

## SUMMARY

**Mammalian oocytes are stored in the ovary, where they are arrested in prophase for prolonged periods. The mechanisms that abrogate the prophase arrest in mammalian oocytes and reinitiate meiosis are not well understood. Here, we identify and characterize an essential pathway for the resumption of meiosis that relies on the protein phosphatase DUSP7. DUSP7-depleted oocytes either fail to resume meiosis or resume meiosis with a significant delay. In the absence of DUSP7, Cdk1/CycB activity drops below the critical level required to reinitiate meiosis, precluding or delaying nuclear envelope breakdown. Our data suggest that DUSP7 drives meiotic resumption by dephosphorylating and thereby inactivating cPKC isoforms. In addition to controlling meiotic resumption, DUSP7 has a second function in chromosome segregation: DUSP7-depleted oocytes that enter meiosis show severe chromosome alignment defects and progress into anaphase prematurely. Altogether, these findings establish the phosphatase DUSP7 as an essential regulator of multiple steps in oocyte meiosis.**

## INTRODUCTION

Mammalian oocytes develop over a long period, spanning up to several decades in humans. Their development starts before birth in the embryo. The oocytes are initially very small and are stored for long periods in the ovary. Periodically, some oocytes become activated. They grow in size and accumulate mRNAs and proteins, which are required for embryo development (Eichenlaub-Ritter and Peschke, 2002). When the oocytes have reached their full size, they are capable of maturing into a fertilizable egg. This maturation is triggered once every menstrual cycle by a surge of luteinizing hormone (LH). The surge of LH leads to the activation of the important cell-cycle regulator Cyclin-dependent kinase 1 in complex with its co-activator Cyclin B (Cdk1/CycB). This complex is also known as the maturation promoting factor (MPF). Upon activation, Cdk1/CycB phosphorylates a large number of targets that drive the reinitiation of meiosis. These factors include proteins of the nuclear lamina, whose phosphorylation triggers nuclear envelope breakdown (NEBD) (Adhikari et al., 2012; Lüscher et al., 1991), as well as spindle assembly factors (Häfner et al., 2014; Maia et al., 2012; Whalley et al., 2015). Because the mechanism of Cdk1/CycB activation in meiosis is similar to the canonical prophase pathway that activates Cdk1/CycB in mitosis, the meiotic arrest is also called prophase arrest (Schmitt and Nebreda, 2002). Several mechanisms restrict Cdk1/CycB activity during prophase arrest in mouse oocytes. The co-activator Cyclin B turns over constantly, and its absence ensures low Cdk1/CycB activity (Ledan et al., 2001; Marangos et al., 2007; Reis et al., 2006). In addition, inhibitory phosphorylations on Cdk1 decrease its activity. These phosphorylations are controlled by a regulatory network that responds to LH. The kinases WEE1 and MYT1 maintain the inhibitory phosphorylations on Cdk1 (Han et al., 2005; Lincoln et al., 2002). The phosphatase CDC25 counteracts them but is inactive during the meiotic arrest (Oh et al., 2010; Perdiguero and Nebreda, 2004). Upon a surge of LH, WEE1 and MYT1 are inactivated (Han and Conti, 2006). This initially activates a small pool of Cdk1/CycB, which subsequently phosphorylates and activates CDC25. This ultimately results in full Cdk1/CycB activation, which is a prerequisite to exit the meiotic arrest.

Failure to exit the meiotic arrest has been implicated in female infertility (Hsieh et al., 2007; Mitri et al., 2014; Richards et al., 2002). Understanding the mechanisms that control meiotic resumption is thus of medical relevance. Current research on meiotic resumption mainly focuses on protein kinases and the protein phosphatases PP1 and PP2A (Adhikari and Liu, 2014; Holt et al., 2013). We recently performed a large-scale RNAi screen to identify genes that are involved in the regulation of mammalian meiosis (Pfender et al., 2015). Through this screen, we identified dual-specificity phosphatase (DUSP) 7 as a phosphatase that is essential for the resumption of meiosis.

DUSP7 is a cytoplasmic phosphatase and was identified as mitogen-activated protein kinase-phosphatase (MKP). DUSP7 is known to dephosphorylate the p42/p44 mitogen-activated protein kinases (p42/p44 MAPKs, better known as ERK1/2), which inactivates them (Caunt et al., 2008). Generally, DUSPs binds to their targets via a conserved arginine-rich kinase interaction motif, which is located amino-terminally of the phosphatase domain (Camps et al., 1998). Little is known about the function of DUSP7. In acute leukemia, DUSP7 is frequently overexpressed (Levy-Nissenbaum et al., 2003), but its physiological role is still unknown.


This is an open access article under the CC BY-NC-ND license (http://creativecommons.org/licenses/by-nc-nd/4.0/).

We show here that DUSP7 is essential for two crucial steps of oocyte meiosis: first, it is required for timely NEBD to facilitate the reinitiation of meiosis; second, it is essential for accurate chromosome segregation. We establish the mechanisms by which DUSP7 fulfills these functions and attribute a physiological role to DUSP7 during development.

## RESULTS

### DUSP7 Depletion in Mouse Oocytes Delays and Prevents Meiotic Resumption

We depleted DUSP7 by culturing small interfering RNA (siRNA)-injected oocytes within follicles in vitro (Figure S1A). This system is particularly well suited to deplete stable proteins in mouse oocytes, because it prevents protein synthesis from an early stage of oocyte growth onward (Pfender et al., 2015). In short, small immature oocytes that are surrounded by cumulus cells (follicles) were isolated from female mice around 11 days after birth. After microinjection with siRNAs against DUSP7 and subsequent culture for 10 days ex vivo, the fully grown and mature oocytes were stripped of the cumulus cells and microinjected a second time with mRNAs encoding fluorescent reporter proteins and rescue constructs. We then followed meiosis by high-resolution live cell microscopy.

First, we verified that our follicle culture system is suitable to study the regulation of cell-cycle events by comparing in vivo and in vitro grown oocytes. In both groups, the activity of the E3 ubiquitin ligase anaphase promoting complex/cyclosome (APC/C) was comparable (Figure S1B). In addition, the levels of important cell-cycle regulators such as the kinase Cdk1 and the phosphatase CDC25B are similar (Figure S1C). This is consistent with our previous study that showed that meiosis progresses in a similar manner in in vitro and in vivo grown oocytes and that the transcriptome of both groups is closely related (Pfender et al., 2015). Altogether, these data suggest that oocytes that were cultured within follicles in vitro are suitable to study the meiotic cell cycle.

DUSP7-depleted oocytes were frequently unable to undergo NEBD, the first visible sign of meiotic resumption (Figures 1A and 1B; Figures S1D–S1G). This phenotype was specifically due to the depletion of DUSP7, because GFP-tagged wild-type DUSP7 ($DUSP7^{wt}$) rescued NEBD. A catalytically inactive version of DUSP7 (C333S, $DUSP7^{c.i.}$) did not rescue NEBD, indicating that the catalytic activity of DUSP7 is essential for its function (Figure 1B). Those DUSP7-depleted oocytes that still underwent NEBD did so with a delay of around 2 hr (Figure 1C). The timing of NEBD in DUSP7-depleted oocytes that expressed GFP-tagged wild-type DUSP7 was still slower than in control oocytes (Figure 1C). This is likely due to a partial rescue by GFP-tagged wild-type DUSP7, which allowed a larger number of oocytes to progress into meiosis (Figure 1B) but did not fully restore the timing of NEBD in these rescued oocytes due to decreased levels of Cdk1/CycB activity, as we discuss in more detail later.

Next, we wanted to identify the targets of DUSP7 that drive the release from prophase arrest. To this end, we created a DUSP7 mutant that can no longer interact with ERK1/2 and tested whether this mutant can rescue the DUSP7 depletion phenotype. The DUSP7 residues that are essential for the interaction with ERK1/2 were not known, but they were previously shown for DUSP6, a close relative of DUSP7 (Tanoue et al., 2002). By sequence alignment, we identified arginine 104 and arginine 105 in the kinase interaction motif of DUSP7 as the likely residues that are essential for the interaction with ERK1/2. We then performed co-immunoprecipitation assays in HeLa cells expressing ERK2, together with the FLAG-tagged DUSP7 mutant (R104/105M, MAPK binding mutant, $DUSP7^{MBM}$) or other FLAG-tagged DUSP7 (FLAG-DUSP7) variants (Figure 1D). $DUSP7^{wt}$ and catalytically inactive DUSP7 bound efficiently to ERK2. In contrast, $DUSP7^{MBM}$ did not bind to ERK2, confirming that we had identified the correct residues (Figure 1D). We then expressed similar levels of wild-type DUSP7, as well as $DUSP7^{MBM}$, in DUSP7-depleted oocytes (Figure S1H). DUSP7-depleted oocytes that expressed $DUSP7^{MBM}$ underwent NEBD with the same high efficiency as oocytes expressing $DUSP7^{wt}$ (Figures 1B and 1C). This indicates that DUSP7's function in NEBD does not require its interaction with ERK1/2. These data are unexpected given that no other targets of DUSP7 besides ERK1/2 are known. However, consistent with this finding, previous studies reported that ERK1/2 are only activated after NEBD in mouse oocytes. This renders a function of ERK1/2 in NEBD unlikely (Choi et al., 1996; Colledge et al., 1994; Verlhac et al., 2000).

### An In Vitro Phospho-peptide Screening Assay Identified cPKC Isoforms as DUSP7 Substrates

We speculated that other, so far unknown substrates of DUSP7 could drive meiotic resumption. To identify these substrates, we carried out an in vitro phospho-peptide screening assay. In this assay, synthetic 12–13 amino acid-long peptides with a phosphorylated serine, threonine, or tyrosine residue are incubated with a phosphatase. If the phosphatase dephosphorylates a peptide, the phosphate moiety is released and detected by a chelating solution that changes color upon phosphate binding. We purified active DUSP7 from bacteria and performed five independent in vitro dephosphorylation assays. We then focused on protein substrates that were found in at least three of the assays (Figure 2A). In this way, we identified Ephrin type-A receptors (Epha), phospholipase C gamma 1 (PLC$\gamma$1), and different conventional protein kinase C (cPKC) isoforms as DUSP7 substrates. RNAi-mediated targeting of these proteins did not result in a detectable phenotype (Figures S2A–S2C). However, previous studies suggested that activation of cPKC isoforms, for example, by Phorbol 12-myristate 13-acetate (PMA), a highly potent activator of cPKC isoforms, delays meiotic resumption in mouse oocytes (Downs et al., 2001; Lefèvre et al., 1992). We confirmed that PMA delays meiotic entry, mimicking the DUSP7 depletion phenotype (Figures 2B–2D). In addition, the specific upregulation of cPKC activity by overexpressing constitutively active $PKC\beta2^{A25E}$ (Hennige et al., 2010) delayed NEBD to a similar extent as DUSP7 depletion (Figures S2D–S2F). Based on these results, we hypothesized that DUSP7 promotes NEBD by dephosphorylating and inactivating cPKC isoforms. Consequently, cPKC isoforms should remain active in the absence of DUSP7. If this hypothesis holds true, inactivation of cPKC isoforms in DUSP7-depleted oocytes should rescue the

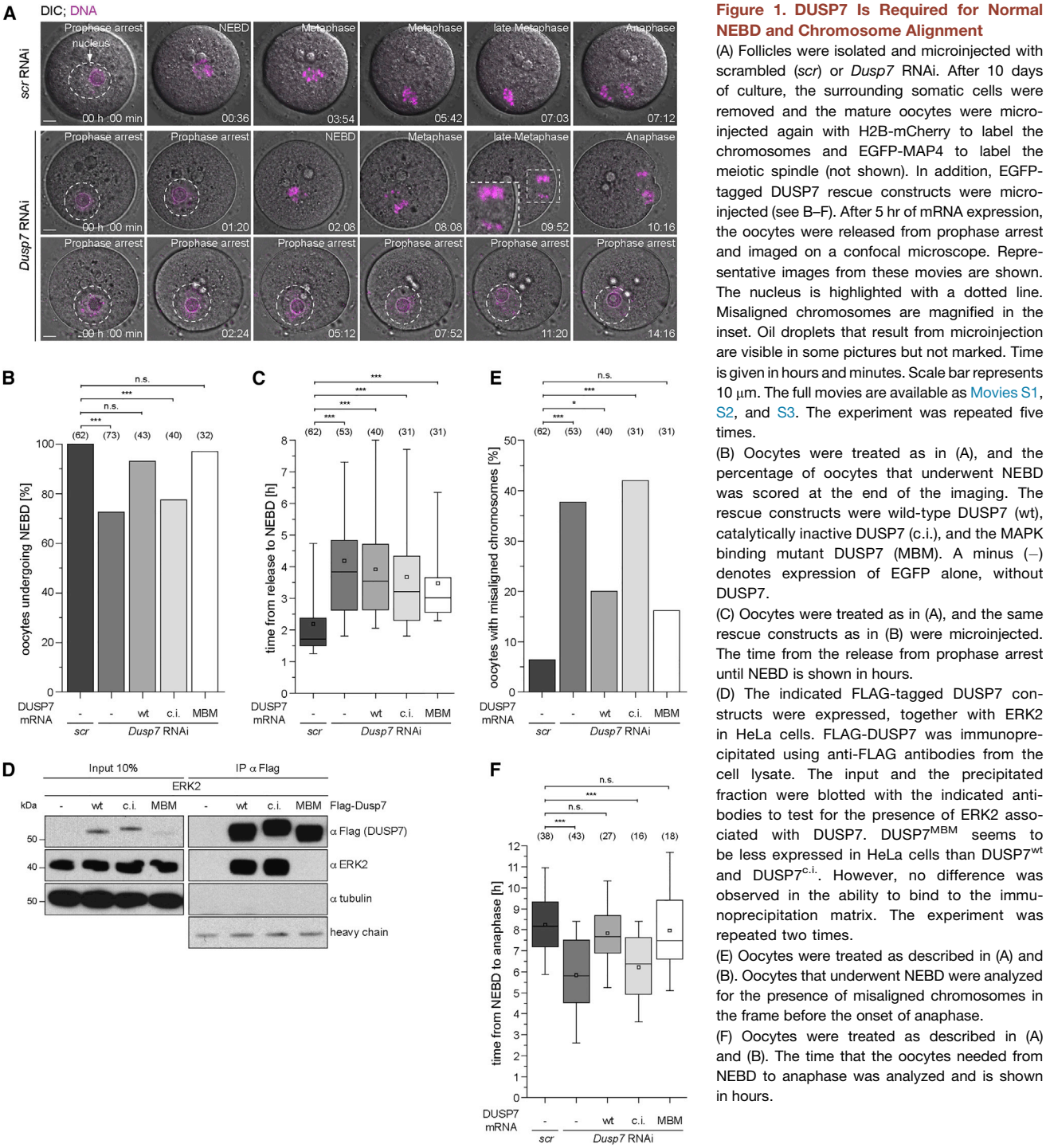


**Figure 1. DUSP7 Is Required for Normal NEBD and Chromosome Alignment**

(A) Follicles were isolated and microinjected with scrambled (*scr*) or *Dusp7* RNAi. After 10 days of culture, the surrounding somatic cells were removed and the mature oocytes were microinjected again with H2B-mCherry to label the chromosomes and EGFP-MAP4 to label the meiotic spindle (not shown). In addition, EGFP-tagged DUSP7 rescue constructs were microinjected (see B–F). After 5 hr of mRNA expression, the oocytes were released from prophase arrest and imaged on a confocal microscope. Representative images from these movies are shown. The nucleus is highlighted with a dotted line. Misaligned chromosomes are magnified in the inset. Oil droplets that result from microinjection are visible in some pictures but not marked. Time is given in hours and minutes. Scale bar represents 10 μm. The full movies are available as Movies S1, S2, and S3. The experiment was repeated five times.

(B) Oocytes were treated as in (A), and the percentage of oocytes that underwent NEBD was scored at the end of the imaging. The rescue constructs were wild-type DUSP7 (wt), catalytically inactive DUSP7 (c.i.), and the MAPK binding mutant DUSP7 (MBM). A minus (–) denotes expression of EGFP alone, without DUSP7.

(C) Oocytes were treated as in (A), and the same rescue constructs as in (B) were microinjected. The time from the release from prophase arrest until NEBD is shown in hours.

(D) The indicated FLAG-tagged DUSP7 constructs were expressed, together with ERK2 in HeLa cells. FLAG-DUSP7 was immunoprecipitated using anti-FLAG antibodies from the cell lysate. The input and the precipitated fraction were blotted with the indicated antibodies to test for the presence of ERK2 associated with DUSP7. $DUSP7^{MBM}$ seems to be less expressed in HeLa cells than $DUSP7^{wt}$ and $DUSP7^{c.i.}$. However, no difference was observed in the ability to bind to the immunoprecipitation matrix. The experiment was repeated two times.

(E) Oocytes were treated as described in (A) and (B). Oocytes that underwent NEBD were analyzed for the presence of misaligned chromosomes in the frame before the onset of anaphase.

(F) Oocytes were treated as described in (A) and (B). The time that the oocytes needed from NEBD to anaphase was analyzed and is shown in hours.

depletion phenotype. We thus treated DUSP7-depleted oocytes with the cPKC inhibitor CGP-53353 (Traxler et al., 1997). Increasing concentrations of the inhibitor partially rescued the number of oocytes that underwent NEBD (Figure 2E). To confirm the specificity of this result, we co-depleted DUSP7 and PKCβ in follicles. In addition, the co-depletion of PKCβ rescued the efficiency of NEBD in DUSP7-depleted oocytes (Figures S2H–S2L). In both rescue conditions, the timing of NEBD was still slower than in controls (Figure 2F; Figure S2I), which is likely due to increased, but overall lower, levels of Cdk1/CycB activity, as we discuss in more detail later.

To demonstrate the physiological relevance of these findings, we tested in vivo whether cPKC activity is increased in DUSP7-depleted oocytes. As a measure of cPKC activity, we used an

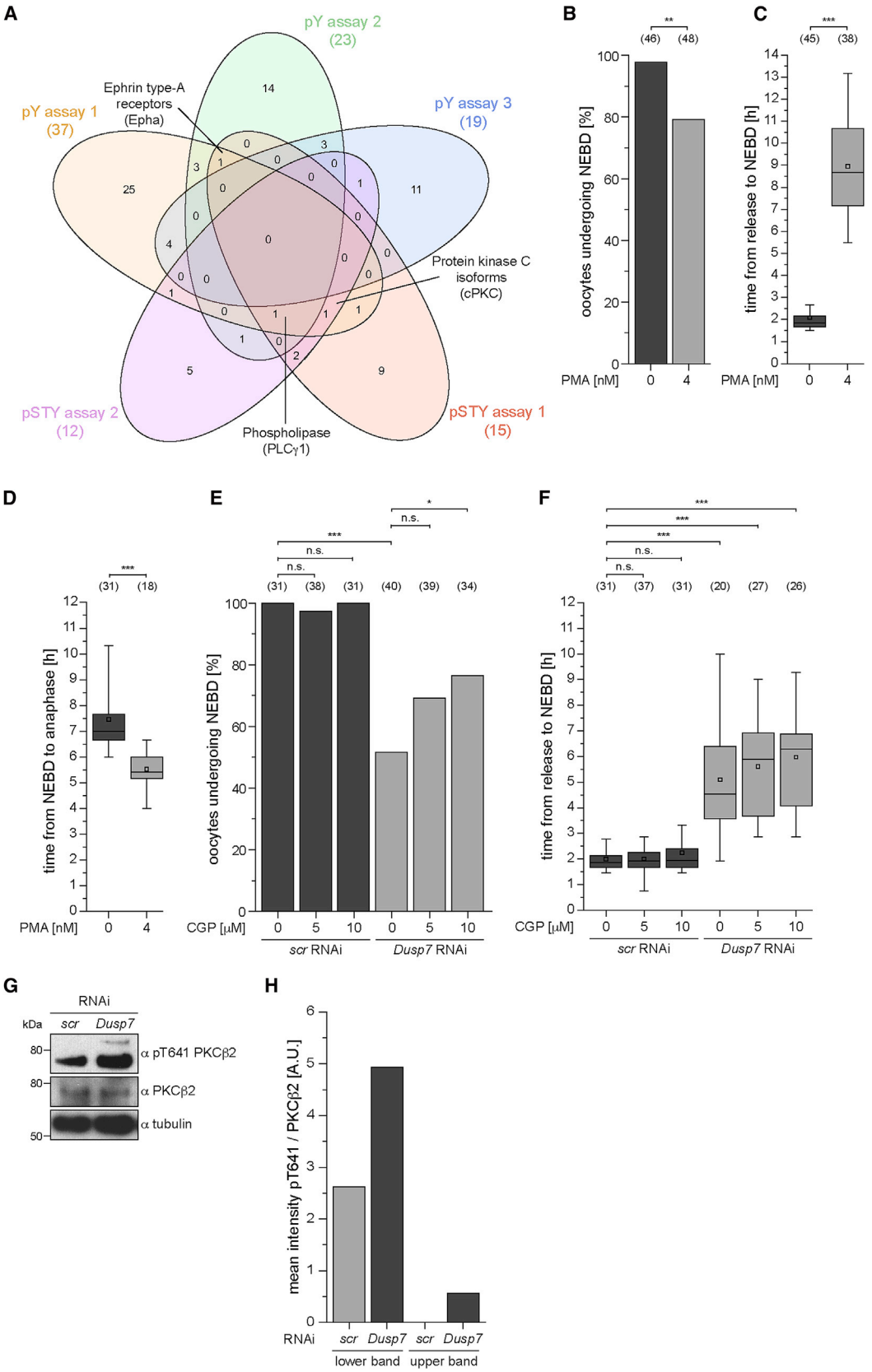


*(legend on next page)*

antibody against auto-phosphorylated cPKC, because the degree of auto-phosphorylation represents an estimate of cPKC activity (Edwards et al., 1999). In particular, we used an antibody specific for phosphorylated threonine 641 of PCKβ2 (pT641), which was also identified as DUSP7 target site by the in vitro phospho-peptide assay. We verified that this antibody is phospho-specific (Figure S2M). We found that the pT641 signal is increased in DUSP7-depleted compared to control-depleted oocytes (Figures 2G and 2H). Moreover, in DUSP7-depleted samples only, we observed a second band above the phospho-PCKβ2 signal, which might represent a highly phosphorylated, active form of cPKC (Edwards et al., 1999). The total protein level of PCKβ2 was unchanged, as judged by immunoblotting with a PKCβ2 antibody (Figure 2G). Collectively, these results establish that DUSP7 dephosphorylates cPKC isoforms in mouse oocytes to facilitate NEBD.

## Restoring Cdk1/CycB Activity in DUSP7-Depleted Oocytes Rescues DUSP7 Depletion

Our in vitro phospho-peptide assay identified cPKC isoforms as DUSP7 targets. However, the mechanism by which DUSP7 depletion causes a prolonged meiotic arrest remained unclear. A prerequisite for NEBD is Cdk1/CycB activation. We speculated that the activity of Cdk1/CycB might be too low to support timely NEBD in DUSP7-depleted oocytes. We tested this hypothesis with a radioactive Cdk1 kinase assay using histone H1 as substrate (Figure 3A; Figure S3A). In particular, we quantified Cdk1/CycB activity in mouse oocytes 6 hr after release from prophase arrest, because the Cdk1/CycB1 activity peaked at this time point in both conditions (Figure S3A). We found that Cdk1/CycB activity is reduced by around 40% in DUSP7-depleted oocytes (Figure 3B). In addition, we performed the assay in the presence of the cPKC activator PMA and observed a similar decrease in Cdk1/CycB activity (Figure 3C). We speculate that in the absence of DUSP7, Cdk1/CycB activity drops below the critical level required to resume meiosis. Expression of GFP-tagged wild-type DUSP7 restores Cdk1/CycB activity to levels that are sufficient to promote NEBD, but the overall level of activity may still be lower than in controls. This might be why $DUSP7^{wt}$ expression or cPKC inhibition or depletion in DUSP7-depleted oocytes rescues the number of oocytes that undergo NEBD but does not restore normal timing of NEBD.

If the DUSP7 depletion phenotype is due to decreased Cdk1/CycB activity, increasing Cdk1/CycB activity should rescue the DUSP7 depletion phenotype. To test this, we artificially increased Cdk1/CycB activity to three levels (Figure 3D). First, we increased the amount of wild-type Cdk1 protein ($Cdk1^{wt}$). This should only result in a mild increase in Cdk1/CycB activity, because the kinases WEE1 and MYT1 still phosphorylate and thereby inhibit $Cdk1^{wt}$ (Han et al., 2005; Oh et al., 2010). Expression of $Cdk1^{wt}$ did not change the percentage of oocytes that underwent NEBD (Figure 3E) but caused a minor reduction in the timing of NEBD in DUSP7-depleted oocytes (Figure 3F). Next, we expressed an active Cdk1 mutant that cannot be phosphorylated by WEE1 and MYT1 (Cdk1 T14A, Y15F: $Cdk1^{AF}$). This should result in a strong increase of Cdk1/CycB activity (Pomerening et al., 2008). Control and DUSP7-depleted oocytes expressing GFP-$Cdk1^{AF}$ underwent NEBD shortly after release from prophase arrest, when EGFP-expressing oocytes were still arrested (Figure 3G). We obtained the same result when we expressed CDC25B, the phosphatase that activates Cdk1/CycB in mouse oocytes (Figure S3B) (Lincoln et al., 2002; Okazaki et al., 1996; Pirino et al., 2009). Both conditions increase Cdk1/CycB activity to very high levels (Figure 3D) and lead to a premature rescue of the DUSP7 depletion phenotype. Finally, we increased Cdk1/CycB activity to intermediate levels by expressing Cyclin B1, the co-activator of Cdk1 (de Vantéry et al., 1997). Expression of mCherry-tagged Cyclin B1 (CycB1-mCherry) in DUSP7-depleted oocytes was able to fully rescue the DUSP7 depletion phenotype. The percentage of oocytes that underwent NEBD and the timing of NEBD were comparable to the results for control oocytes (Figures 3I and 3J). This suggests that decreased Cdk1/CycB activity is the cause for the delay of NEBD in DUSP7-depleted oocytes.

## The Spindle Assembly Checkpoint Is Compromised in DUSP7-Depleted Oocytes

DUSP7 depletion caused a second prominent phenotype, in addition to impairing meiotic resumption: the DUSP7-depleted oocytes that underwent NEBD often had misaligned chromosomes close to anaphase (Figures 1A, inset, and 1E). In addition,

**Figure 2. Inactivation of cPKC Isoforms Rescues DUSP7 Depletion**

(A) Venn diagram showing the distribution of hits from five independent in vitro phospho-peptide screening assays. Intersections between two or more assays show hits that were found in all these assays. Proteins that were found in at least three assays are highlighted.

(B) Mature oocytes were isolated and microinjected with H2B-mCherry and EGFP-MAP4. After mRNA expression, the oocytes were released in the presence of DMSO or PMA and imaged on a confocal microscope. The percentage of oocytes that underwent NEBD was scored at the end of the imaging. The experiment was repeated four times.

(C) Oocytes from (B) were analyzed for the time (in hours) from release from prophase arrest to NEBD.

(D) Oocytes from (B) that underwent NEBD were analyzed for the time spent between NEBD and anaphase.

(E) Follicles were isolated and microinjected with scrambled (*scr*) or *Dusp7* RNAi and cultured. The mature oocytes were microinjected a second time with H2B-mCherry and EGFP-MAP4. After mRNA expression, the oocytes were released in the presence of DMSO or the indicated concentrations of the cPKC inhibitor CGP-53353 and imaged on a confocal microscope. The percentage of oocytes that underwent NEBD was scored at the end of the imaging. The experiment was repeated five times.

(F) Oocytes from (E) were analyzed for their time from release from prophase arrest to NEBD.

(G) Follicles were treated as described in (E) but not microinjected a second time. The oocytes were lysed in Laemmli sample buffer and blotted for the indicated proteins. For the *scr* RNAi-treated lane, 18 oocytes were used; for the *Dusp7* RNAi group, 21 oocytes were used.

(H) The mean intensities of the pT641 PKCβ2 and the PKCβ2 bands from the immunoblot shown in (G) were quantified. The ratio of the lower band and the upper band in the pT641 PKCβ2 blot to the PKCβ2 band was calculated and is shown.

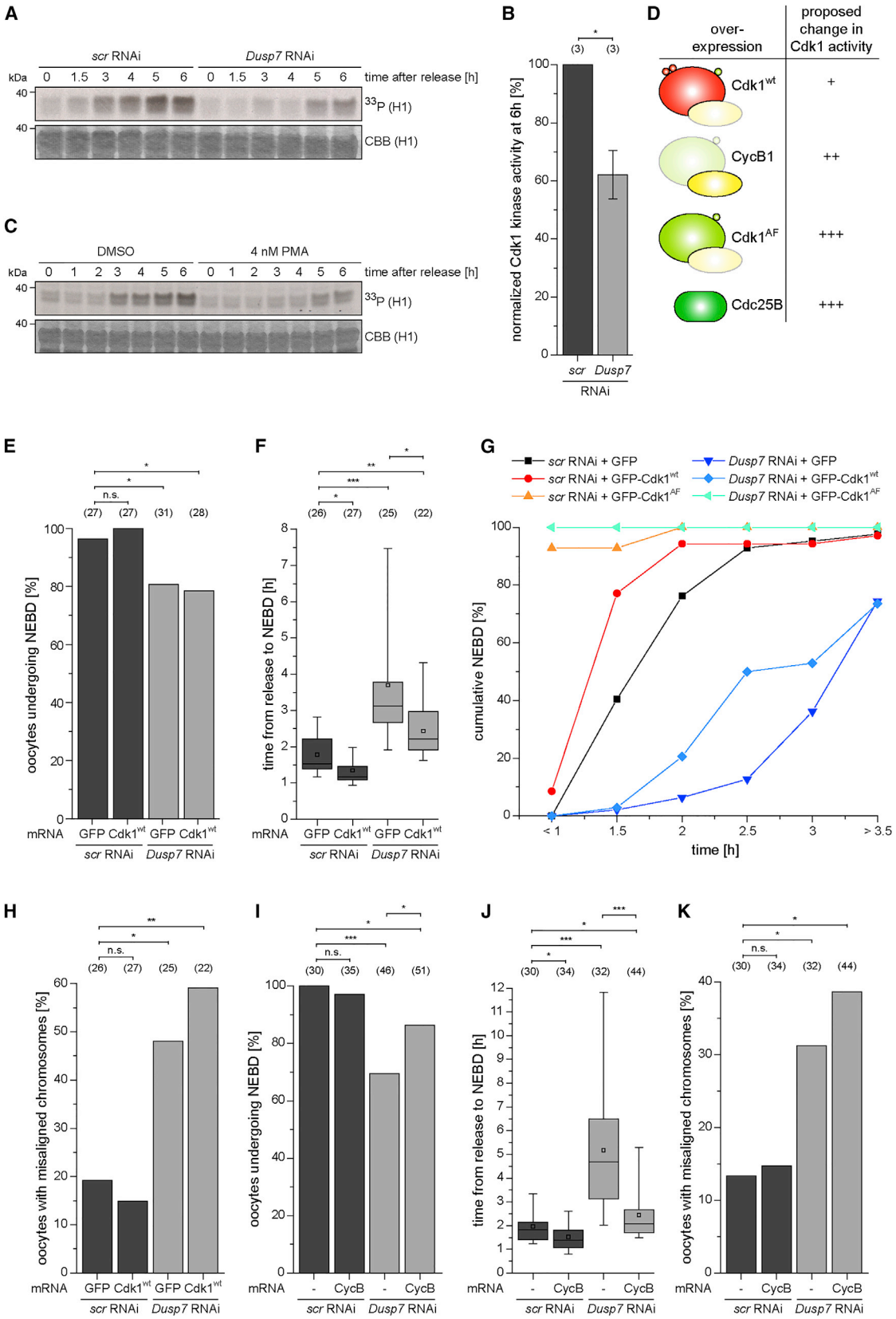


*(legend on next page)*

the time from NEBD to anaphase was drastically shortened (Figure 1F). These defects were specifically due to the depletion of DUSP7, because expression of wild-type (DUSP7$^{wt}$) or ERK1/2 binding deficient (DUSP7$^{MBM}$) DUSP7 partially rescued both defects (Figures 1E and 1F). The rescue required the catalytic activity of DUSP7, because catalytically inactive DUSP7 (DUSP7$^{c.i.}$) did not rescue the defects (Figures 1E and 1F).

Chromosome alignment at the metaphase plate is preceded by the attachment of kinetochores to spindle microtubules. The spindle assembly checkpoint (SAC) delays anaphase onset in response to unattached chromosomes by generating an inhibitory signal (Kouznetsova et al., 2014; Touati and Wassmann, 2016; Wassmann et al., 2003). The kinetochore localized kinases MPS1 and Aurora B participate in both steps to promote the correct attachment and alignment of chromosomes on the metaphase plate. Inhibition of MPS1 has been reported to lead to chromosome misalignment and premature anaphase onset in mouse oocytes (Hached et al., 2011; Nijenhuis et al., 2014). Given that the depletion of DUSP7 results in chromosome misalignment and premature progression into anaphase, we investigated whether SAC signaling could be impaired in the absence of DUSP7. To test this possibility, we overexpressed a core component of the SAC: MAD1 (SNAP-tagged MAD1, SNAP-MAD1). MAD1 localizes to the kinetochores of unattached chromosomes, where it catalyzes the generation of the inhibitory signal (Kulukian et al., 2009; Sironi et al., 2001). Overexpression of SAC components in mouse oocytes causes a metaphase arrest independently of misaligned chromosomes if the SAC is functional (Wassmann et al., 2003). As the SAC component, we decided to overexpress SNAP-MAD1, because it is also suitable to mark kinetochores of misaligned chromosomes by live cell microscopy (Chmátal et al., 2015). The expression of SNAP-MAD1 in control or DUSP7-depleted oocytes did not influence the number of oocytes undergoing NEBD or the timing of NEBD (Figures S4A and S4B). As expected, control oocytes expressing SNAP-MAD1 arrested in metaphase (Figure 4B). In contrast, DUSP7-depleted oocytes expressing SNAP-MAD1 did not arrest in metaphase but progressed into anaphase after a delay (Figure 4B; Figure S4C).

We then investigated the localization of SAC proteins. Control oocytes, as well as DUSP7-depleted oocytes, showed a positive SNAP-MAD1 signal at kinetochores shortly after NEBD (Figure 4A; Figure S4D). This confirms that the initial recruitment of SAC components to the kinetochore is not altered in the absence of DUSP7. Misaligned chromosomes in control oocytes are rare and can only be observed transiently upon formation of a metaphase plate in control oocytes (Chmátal et al., 2015). However, previous studies showed that they are positive for MAD1 (Chmátal et al., 2015; Zhang et al., 2005). Consistent with these studies, 81% (9 of 11 recordings) of misaligned chromosomes in 33 control oocytes were positive for MAD1 (Figure S4E). By contrast, only 26% (5 of 19 recordings) of misaligned chromosomes in 28 DUSP7-depleted oocytes were positive for MAD1 (Figure S4E). These data suggest that SAC proteins are not efficiently retained at misaligned kinetochores in the absence of DUSP7. If this holds true, inactivating the SAC by other means should show a similar phenotype. Inhibition of the kinase MPS1 is known to disturb SAC signaling in mouse oocytes, and the oocytes progress into anaphase in the presence of misaligned chromosomes (Hached et al., 2011). Depletion of DUSP7 or MPS1 resulted in a similar time from NEBD to anaphase (Figure 4C). Co-depletion of MPS1 in DUSP7-depleted oocytes reduced the time of anaphase further, possibly due to a more complete inactivation of the checkpoint (Figure 4C). Both MPS1 and DUSP7 depletion caused chromosome alignment defects. The percentage of oocytes with misaligned chromosomes was higher in MPS1-depleted oocytes than in DUSP7-depleted oocytes and did not increase further upon co-depletion (Figure 4D). The number of oocytes undergoing NEBD and the time from release to NEBD were not influenced by MPS1 depletion (Figures S4F and S4G). However, the overall phenotypes were similar, consistent with impaired SAC signaling in DUSP7-depleted oocytes.

**Figure 3. Increased Cdk1/CycB Activity Rescues DUSP7 Depletion**

(A) Follicles were depleted of DUSP7 or microinjected with scrambled (*scr*) RNAi. After culture, the oocytes were released and snap frozen at the indicated time points. The auto-radiogram shows the incorporation of radioactive phosphate into histone H1. Coomassie brilliant blue (CBB) staining shows histone H1.

(B) The intensity of the radioactive histone H1 signal at 6 hr after release was measured and normalized to histone H1 protein. The experiment was repeated three times.

(C) Mature oocytes were isolated and released in the presence of either DMSO or the cPKC activator PMA. Oocytes were snap frozen at the indicated time points. The auto-radiogram shows the incorporation of radioactive phosphate into histone H1. CBB staining shows histone H1.

(D) Scheme showing the different constructs to modulate Cdk1/CycB kinase activity and the expected relative increase of Cdk1/CycB activity. A + sign indicates a mild increase, ++ indicates a medium increase and +++ stands for Cdk1/CycB hyper-activation.

(E) Follicles were depleted as described in (A) but microinjected a second time after isolation with H2B-mCherry and GFP or GFP-Cdk1 wild-type (Cdk1$^{wt}$). After mRNA expression, the oocytes were released and imaged on a confocal microscope. The percentage of oocytes that underwent NEBD was scored at the end of the imaging. The experiment was repeated three times.

(F) Follicles were treated as in (E), and the time from release from prophase arrest to NEBD was measured.

(G) Follicles were treated as in (E). GFP-tagged hyper-active Cdk1 (Cdk1$^{AF}$) was microinjected in a separate group of oocytes. This group underwent NEBD before imaging at the microscope was started, and analysis of the timing was therefore not possible. Instead, all oocytes that underwent NEBD within a time frame of 60 min after release (and within 30 min intervals afterward) were grouped together. The cumulative percentage of oocytes that underwent NEBD after the indicated time is shown.

(H) Oocytes from (E) that performed NEBD were analyzed for the presence of misaligned chromosomes in the frame before the onset of anaphase.

(I) Follicles were treated as in (E) but microinjected with H2B-mCherry and CycB1-mCherry. After mRNA expression, the oocytes were released and imaged on a confocal microscope. The percentage of oocytes that underwent NEBD was scored at the end of the imaging. The experiment was repeated five times.

(J) Oocytes from (I) were analyzed for the time from release from prophase arrest to NEBD.

(K) Oocytes from (I) that performed NEBD were analyzed for the presence of misaligned chromosomes in the frame before the onset of anaphase.

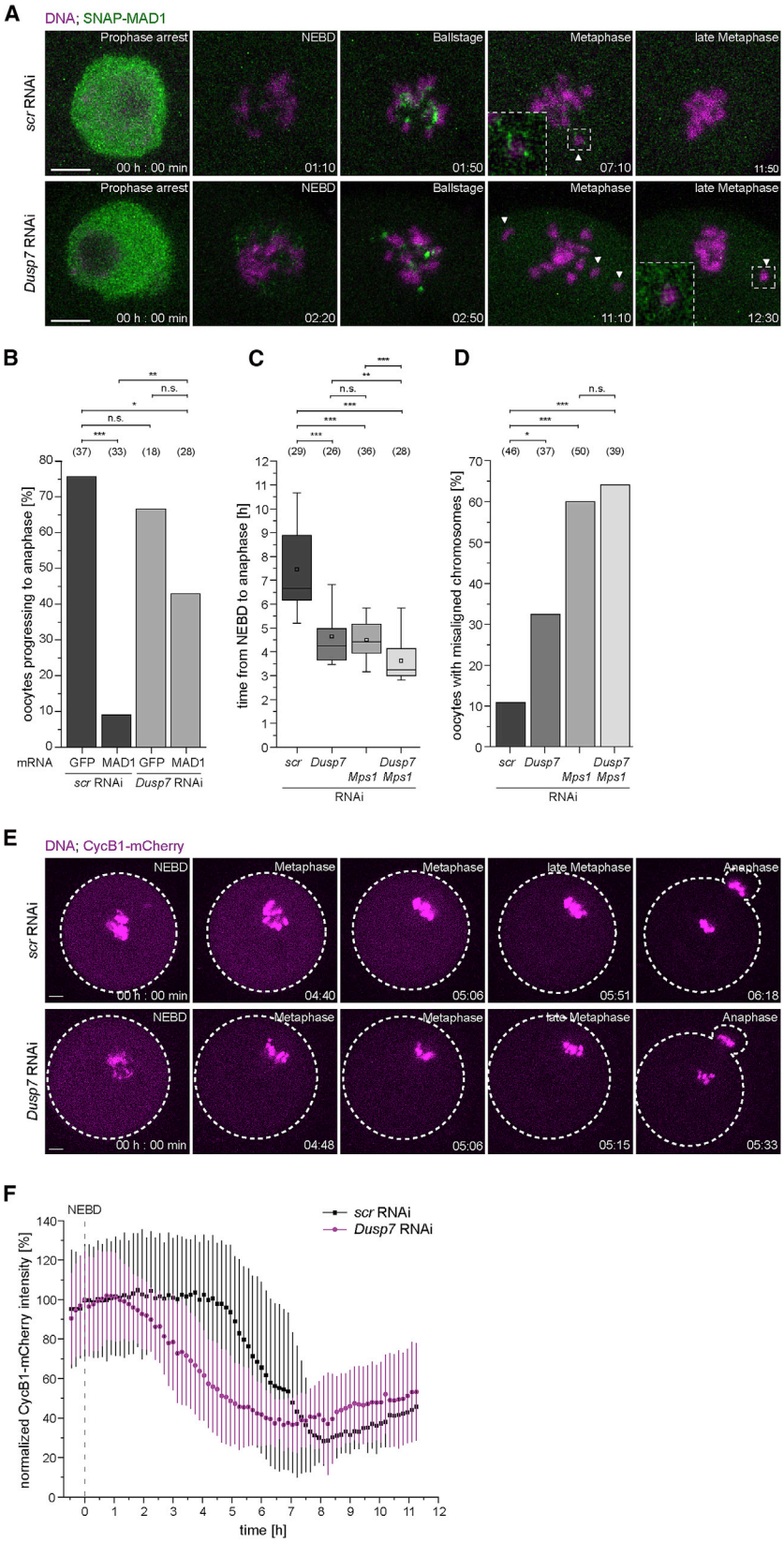


**Figure 4. DUSP7 Participates in the SAC Response in Mouse Oocytes**

(A) Follicles were microinjected with scrambled (*scr*) or *Dusp7* RNAi and cultured. The somatic cells were removed and the oocytes were microinjected a second time with H2B-mCherry to mark the chromosomes and SNAP-tagged MAD1 (SNAP-MAD1). After mRNA expression, the SNAP tag was labeled with SNAP-Cell 505 Star. The oocytes were released and imaged on a confocal microscope. Representative images of these movies are shown. Misaligned chromosomes are highlighted with white arrowheads. Time is given in hours and minutes. Scale bar represents 10 μm. The inset shows a magnification of one misaligned chromosome per group. The channel for SNAP-MAD1 in the inset was adjusted in brightness to visualize MAD1 better. The full movies are available as Movies S4 and S5. The experiment was repeated four times.

(B) Oocytes from (A) and additional oocytes treated in the same way but microinjected with EGFP alone were analyzed for their progression into anaphase.

(C) Follicles were microinjected with scrambled (*scr*), *Dusp7*, and/or *Mps1* siRNAs and cultured. The oocytes were microinjected with H2B-mCherry and EGFP-MAP4. After mRNA expression, the oocytes were released and imaged on a confocal microscope. Their time from release from prophase arrest to anaphase was analyzed. The experiment was repeated four times.

(D) The same oocytes as in (C) were analyzed for the presence of misaligned chromosomes in the last frame before anaphase.

(E) Representative images from oocytes used in Figure 3I to illustrate the earlier onset of CycB1-mCherry degradation in DUSP7-depleted oocytes.

(F) The CycB1-mCherry fluorescence was measured in oocytes from Figure 3I as described in Lane and Jones (2014). The average fluorescence intensity at NEBD was set to 100%.

A key target in SAC signaling is the APC/C. The APC/C is a multi-subunit ubiquitin ligase that regulates the onset of anaphase by targeting the anaphase inhibitor securin and other M-phase substrates for degradation (Barford, 2011; Primorac and Musacchio, 2013). The SAC delays anaphase by inhibiting the APC/C until the chromosomes are correctly attached to the spindle. If SAC signaling is compromised in DUSP7-depleted oocytes, the APC/C should be inefficiently inhibited. Therefore, the APC/C should trigger the degradation of its substrates earlier than under normal conditions. A well-known substrate of the APC/C is CycB1, the co-activator of Cdk1. We expressed CycB1-mCherry in control and DUSP7-depleted oocytes (Figures 4E and 4F). As predicted, the APC/C was activated earlier in DUSP7-depleted oocytes, as reflected by a significantly earlier onset of CycB1-mCherry degradation.

The decreased activity of the SAC could also be a consequence of the lower Cdk1/CycB activity that we observed in DUSP7-depleted oocytes (Figure 3A) (Clijsters et al., 2014; McCloy et al., 2014; Rattani et al., 2014). However, upregulation of Cdk1/CycB activity or inhibition of cPKC isoforms did not restore normal chromosome alignment in DUSP7-depleted oocytes (Figures 3H and 3K; Figures S2G and S2J). In addition, the time from NEBD to anaphase was not rescued when Cdk1/CycB activity was increased (Figures S2K, S3C, and S3D). These results suggest that the defects in SAC signaling are not solely due to a decrease in Cdk1/CycB in the absence of DUSP7.

## DISCUSSION

The tight and reliable control of meiotic resumption is crucial for reproduction. Although defects in meiotic resumption have been implicated in infertility (Hsieh et al., 2007; Hunt and Hassold, 2008; Mitri et al., 2014; Richards et al., 2002), the molecular mechanisms that drive the reinitiation of meiosis are still incompletely understood. Our results provide mechanistic insights into how the prophase arrest in oocytes is abrogated.

We identified an unexpected signaling pathway that is essential for the release from prophase arrest. In this pathway, DUSP7 drives meiotic resumption by dephosphorylating and thereby inactivating cPKC isoforms, which is essential for timely NEBD. This pathway is likely to be crucial for meiosis, because a DUSP7 knockout mouse created by the International Mouse Phenotyping Consortium has been reported to be infertile. The DUSP7-dependent pathway could act in parallel to the canonical Cdk1/CycB activation mechanism that has been implicated in the release from prophase arrest. In the canonical pathway, cyclic AMP-activated protein kinase A (PKA) activates WEE1, which inhibits Cdk1/CycB and thereby prevents meiotic resumption (Han and Conti, 2006; Oh et al., 2010). After the LH surge, PKA and consequently WEE1 are inactivated and Cdk1/CycB becomes active. Having two parallel pathways that control meiotic resumption may allow oocytes to trigger the release from prophase arrest more robustly and to integrate more signals before oocytes are allowed to resume meiosis. This may reduce the risk of precocious meiotic resumption and increase the chance of conception.

DUSP7 promotes the release from prophase arrest by dephosphorylating and thereby inhibiting cPKC isoforms, a prerequisite for the timely activation of Cdk1/CycB. But what is the link between cPKC isoforms and Cdk1/CycB? Protein kinase C (PKC) $\alpha$ and PKC$\delta$ are known to regulate the Cdk inhibitors p21(CIP) and p27(Kip1) (Detjen et al., 2000; Frey et al., 1997). p21(CIP) controls the G2/M transition in mouse spermatogenesis (Kaushal and Bansal, 2007), and p27(Kip1) is required for prophase arrest in *Drosophila* oogenesis (Hong et al., 2003). It is thus conceivable that DUSP7 could regulate Cdk1/CycB activity by suppressing an inhibitor of Cdk1/CycB, such as p21 and p27, via cPKC isoforms. In addition, cPKC isoforms can influence the activity of the Cdk1/CycB-activating phosphatase CDC25. They can do so by regulating the activity of CDC25 directly (Yano et al., 2013) or by suppressing its expression (Yoshida et al., 2001). DUSP7 may thus be essential for the timely activation of CDC25.

In addition to a delay or a block in NEBD, we frequently observed misaligned chromosomes and premature progression into anaphase in oocytes depleted of DUSP7 (Figure 4). The SAC arrests mouse oocytes in metaphase until the chromosomes are attached to the meiotic spindle (Wassmann et al., 2003). However, evidence suggests that the SAC in mammalian oocytes is not as stringent as in mitotic cells and some misaligned chromosomes might remain undetected (Kitajima et al., 2011; Kolano et al., 2012; LeMaire-Adkins et al., 1997; Pfender et al., 2015; Zielinska et al., 2015). Many proteins that participate in the SAC are regulated by phosphorylation (Funabiki and Wynne, 2013; London and Biggins, 2014). Consequently, protein phosphatases play a major role in regulating SAC signaling. For example, protein phosphatase 1 removes the phosphorylation on the kinetochore component KNL1 to facilitate stable microtubule attachments and SAC silencing (Liu et al., 2010). In contrast, BubR1 needs to remain phosphorylated to recruit PP2A-B56, which in turn helps to stabilize microtubule attachments (Suijkerbuijk et al., 2012). It is tempting to speculate that DUSP7 contributes to some of these processes. In our in vitro phospho-peptide screen, we did not detect SAC components as potential DUSP7 substrates, even though some were included in the assay (e.g., components of the RZZ complex). We also did not observe a localization of DUSP7 to kinetochores. Instead, DUSP7 remained cytoplasmic in all cell-cycle phases (Pfender et al., 2015). This could suggest that DUSP7 participates not directly in the SAC but indirectly, for example, by regulating other protein kinases or phosphatases.

Alternatively, a weakened SAC response in DUSP7-depleted oocytes could be a consequence of decreased Cdk1/CycB activity (Clijsters et al., 2014; McCloy et al., 2014; Rattani et al., 2014). It was shown that lowering Cdk1/CycB activity leads to an earlier onset of anaphase, even in the presence of misaligned chromosomes. Increasing Cdk1/CycB activity in bub1$^{\Delta/\Delta}$ mice (Rattani et al., 2014) restored the function of the SAC but required a non-degradable version of Cyclin B, artificially enhancing Cdk1/CycB activity. We were able to rescue the timing of NEBD in the absence of DUSP7 by increasing Cdk1/CycB activity using wild-type Cyclin B1 but could not restore a normal SAC response. While these results indicate that the decrease in Cdk1/CycB activity is not the primary cause of the impaired SAC response in the absence of DUSP7, a further increase in Cdk1/CycB activity might restore a normal SAC function.

DUSP7 is also expressed in human oocytes (Madissoon et al., 2014; Zhang et al., 2009), suggesting that its function may be preserved. An important factor that contributes to female infertility in humans is the inability of an oocyte to resume meiosis (Albertini et al., 2003; Hunt and Hassold, 2008; Hutt and Albertini, 2007). It is likely that the malfunction of proteins that are only essential in the oocyte, not in other parts of the body, contributes to this defect. DUSP7 is an excellent candidate for such a protein, because DUSP7 mutant mice are viable but infertile, suggesting that DUSP7 functions primarily in the germline. Analysis of DUSP7's function in humans will be crucial for understanding whether this pathway for meiotic resumption is conserved and whether defects in DUSP7 could contribute to infertility.

## EXPERIMENTAL PROCEDURES

### Preparation and Culture of Follicles, RNAi Sequences, and Drug Treatment of Oocytes

All mice were maintained in a specific pathogen-free environment according to UK Home Office regulations. The work with mice was carried out at the Medical Research Council (MRC) Laboratory of Molecular Biology following the specifications of the UK Home Office. The project license was approved by the UK Home Office and evaluated by the MRC Cambridge Ethics Committee. The preparation of follicles and their culture is described in Pfender et al. (2015). RNAi depletion was performed for 10 days using a final concentration of 50 nM short interfering RNA oligonucleotide (oligo) in the oocyte. The RNAi oligo sequences for DUSP7, Epha4, and Mps1 are described in Pfender et al. (2015). PLC$\gamma$1 was depleted with an oligo mix targeting the sequences 5′-ACGGAAGACCTTCCAGGTCAA-3′, 5′-CCGGGCTGAGGGAAAGATCAA-3′, 5′-CACCGTCATGACTTTGTTCTA-3′, and 5′-CAGGAGGAAGATCCTTATTAA-3′. PKC$\beta$ isoforms 1 and 2 were depleted with an oligo mix targeting the sequences 5′-AAGGACCCTGATTCTACATTA-3′, 5′-CCAGTCAATCATGGAACACAA-3′, 5′-CTGCTGCTTTGTTGTACACAA-3′, and 5′-CCGGAGCAAACACAAGTTTAA-3′. All RNAi oligos were obtained from QIAGEN.

Oocytes treated with PMA or CGP-53353 (Sigma) were incubated with the drug for 1 hr before release. During release and imaging, the drug was still present.

### Confocal Microscopy and Image Preparation

Confocal microscopy was performed as described in Pfender et al. (2015). All oocytes were recorded at least for 14 hr. For some movies, a Leica SP8 inverted confocal microscope equipped with a heated environmental chamber and a motorized stage was used. Imaging was performed with a Leica 40×/1.1 numerical aperture (NA) water immersion objective.

All movies were analyzed and prepared using ImageJ (NIH) and Photoshop (Adobe). If the contrast or the brightness were adjusted, the procedure was applied to the whole image or image sequence. The intensity of bands from auto-radiograms or immunoblots was measured using ImageJ and corrected for background signal and loading control.

### mRNA Preparation and Injection

mRNA was prepared with the mMessage mMachine Kit (Ambion), precipitated with LiCl, and taken up in 20 $\mu$L of RNase-free water. Quantitative microinjection was performed as described (Jaffe et al., 2009). After injection of mRNAs into oocytes, expression was performed for at least 4 hr at 37°C.

### Immunoblotting

All samples were mixed with NuPAGE sample loading buffer (Invitrogen) and heated at 95°C for 5 min. Antibodies used for western blotting were anti-FLAG M2 (mouse, Sigma), anti-ERK2 (rabbit, Santa Cruz), anti-$\alpha$-tubulin (rat, AbD Serotec), anti-PKC$\beta$2 C-terminal (rabbit, Santa Cruz), anti-CDK1 (mouse, Santa Cruz), anti-CDC25B (rabbit, Cell Signaling Technology), and anti-pT641 PKC$\alpha$/$\beta$2 (rabbit, Cell Signaling Technology). All primary antibodies were used in 5% dry milk in PBS with 0.1% Tween 20 and incubated overnight at 4°C. Horseradish peroxidase-coupled secondary anti-mouse (Dako), anti-rabbit (Fisher), and anti-rat (Santa Cruz) antibodies were detected by enhanced chemiluminescence (ECL select, GE Healthcare) and Biomark X-ray (Carestream) or Super RX-N (Fujifilm) films.

### Statistical Analysis

All diagrams were generated using Origin 8 Pro (Origin Software). Boxplots show the first to third quartiles; the median is indicated by a line and the mean is indicated by a square. Error bars on the boxplot denote the 5$^{th}$ and 95$^{th}$ percentiles. For all data shown as boxplots, a two-tailed Student's t test was performed to determine significance. To test significance for all data shown in bar graphs, a Fisher's exact test was performed. One star indicates significance smaller than $5 \times 10^{-2}$, two stars indicate significance smaller than $1 \times 10^{-3}$, and three stars indicate significance smaller than $1 \times 10^{-4}$. All experiments were repeated at least two times, and each number in brackets above the graphs denotes the number of all oocytes used for the analysis, except in Figure 3B and Figures S1A, S2L, and S4D, where the number of experiments is given.

## SUPPLEMENTAL INFORMATION

Supplemental Information includes Supplemental Experimental Procedures, four figures, one table, five movies, and one data file and can be found with this article online at http://dx.doi.org/10.1016/j.celrep.2016.10.007.

## AUTHOR CONTRIBUTIONS

T.T. performed and analyzed all experiments; T.T. and M.S. planned the experiments, discussed the results, and wrote the manuscript. M.S. supervised the study.

## ACKNOWLEDGMENTS

The authors thank all members of the M.S. lab for their input and fruitful discussions. We also acknowledge the biomedical services team of the MRC Laboratory of Molecular Biology and ARES for help with all mice-related questions and for the breeding of our mice. We thank the imaging facility of the LMB for advice on microscopy. T.T. is supported by an EMBO long-term fellowship (ALTF700-2014). The research leading to these results has received financial support from the European Research Council under grant 337415. The work was also supported by the Medical Research Council (MC_U105192711) and the Max Planck Society.

Received: May 16, 2016
Revised: July 29, 2016
Accepted: October 3, 2016
Published: October 25, 2016

## REFERENCES

Adhikari, D., and Liu, K. (2014). The regulation of maturation promoting factor during prophase I arrest and meiotic entry in mammalian oocytes. Mol. Cell. Endocrinol. *382*, 480–487.

Adhikari, D., Zheng, W., Shen, Y., Gorre, N., Ning, Y., Halet, G., Kaldis, P., and Liu, K. (2012). Cdk1, but not Cdk2, is the sole Cdk that is essential and sufficient to drive resumption of meiosis in mouse oocytes. Hum. Mol. Genet. *21*, 2476–2484.

Albertini, D.F., Sanfins, A., and Combelles, C.M. (2003). Origins and manifestations of oocyte maturation competencies. Reprod. Biomed. Online *6*, 410–415.

Barford, D. (2011). Structure, function and mechanism of the anaphase promoting complex (APC/C). Q. Rev. Biophys. *44*, 153–190.

Camps, M., Nichols, A., Gillieron, C., Antonsson, B., Muda, M., Chabert, C., Boschert, U., and Arkinstall, S. (1998). Catalytic activation of the phosphatase MKP-3 by ERK2 mitogen-activated protein kinase. Science *280*, 1262–1265.

Caunt, C.J., Armstrong, S.P., Rivers, C.A., Norman, M.R., and McArdle, C.A. (2008). Spatiotemporal regulation of ERK2 by dual specificity phosphatases. J. Biol. Chem. *283*, 26612–26623.

Chmátal, L., Yang, K., Schultz, R.M., and Lampson, M.A. (2015). Spatial regulation of kinetochore microtubule attachments by destabilization at spindle poles in meiosis I. Curr. Biol. *25*, 1835–1841.

Choi, T., Fukasawa, K., Zhou, R., Tessarollo, L., Borror, K., Resau, J., and Vande Woude, G.F. (1996). The Mos/mitogen-activated protein kinase (MAPK) pathway regulates the size and degradation of the first polar body in maturing mouse oocytes. Proc. Natl. Acad. Sci. USA *93*, 7032–7035.

Clijsters, L., van Zon, W., Riet, B.T., Voets, E., Boekhout, M., Ogink, J., Rumpf-Kienzl, C., and Wolthuis, R.M. (2014). Inefficient degradation of cyclin B1 reactivates the spindle checkpoint right after sister chromatid disjunction. Cell Cycle *13*, 2370–2378.

Colledge, W.H., Carlton, M.B., Udy, G.B., and Evans, M.J. (1994). Disruption of c-mos causes parthenogenetic development of unfertilized mouse eggs. Nature *370*, 65–68.

de Vantéry, C., Stutz, A., Vassalli, J.D., and Schorderet-Slatkine, S. (1997). Acquisition of meiotic competence in growing mouse oocytes is controlled at both translational and posttranslational levels. Dev. Biol. *187*, 43–54.

Detjen, K.M., Brembeck, F.H., Welzel, M., Kaiser, A., Haller, H., Wiedenmann, B., and Rosewicz, S. (2000). Activation of protein kinase Calpha inhibits growth of pancreatic cancer cells via p21(cip)-mediated G(1) arrest. J. Cell Sci. *113*, 3025–3035.

Downs, S.M., Cottom, J., and Hunzicker-Dunn, M. (2001). Protein kinase C and meiotic regulation in isolated mouse oocytes. Mol. Reprod. Dev. *58*, 101–115.

Edwards, A.S., Faux, M.C., Scott, J.D., and Newton, A.C. (1999). Carboxyl-terminal phosphorylation regulates the function and subcellular localization of protein kinase C betaII. J. Biol. Chem. *274*, 6461–6468.

Eichenlaub-Ritter, U., and Peschke, M. (2002). Expression in in-vivo and in-vitro growing and maturing oocytes: focus on regulation of expression at the translational level. Hum. Reprod. Update *8*, 21–41.

Frey, M.R., Saxon, M.L., Zhao, X., Rollins, A., Evans, S.S., and Black, J.D. (1997). Protein kinase C isozyme-mediated cell cycle arrest involves induction of p21(waf1/cip1) and p27(kip1) and hypophosphorylation of the retinoblastoma protein in intestinal epithelial cells. J. Biol. Chem. *272*, 9424–9435.

Funabiki, H., and Wynne, D.J. (2013). Making an effective switch at the kinetochore by phosphorylation and dephosphorylation. Chromosoma *122*, 135–158.

Hached, K., Xie, S.Z., Buffin, E., Cladière, D., Rachez, C., Sacras, M., Sorger, P.K., and Wassmann, K. (2011). Mps1 at kinetochores is essential for female mouse meiosis I. Development *138*, 2261–2271.

Häfner, J., Mayr, M.I., Möckel, M.M., and Mayer, T.U. (2014). Pre-anaphase chromosome oscillations are regulated by the antagonistic activities of Cdk1 and PP1 on Kif18A. Nat. Commun. *5*, 4397.

Han, S.J., and Conti, M. (2006). New pathways from PKA to the Cdc2/cyclin B complex in oocytes: Wee1B as a potential PKA substrate. Cell Cycle *5*, 227–231.

Han, S.J., Chen, R., Paronetto, M.P., and Conti, M. (2005). Wee1B is an oocyte-specific kinase involved in the control of meiotic arrest in the mouse. Curr. Biol. *15*, 1670–1676.

Hennige, A.M., Heni, M., Machann, J., Staiger, H., Sartorius, T., Hoene, M., Lehmann, R., Weigert, C., Peter, A., Bornemann, A., et al. (2010). Enforced expression of protein kinase C in skeletal muscle causes physical inactivity, fatty liver and insulin resistance in the brain. J. Cell. Mol. Med. *14*, 903–913.

Holt, J.E., Lane, S.I., and Jones, K.T. (2013). The control of meiotic maturation in mammalian oocytes. Curr. Top. Dev. Biol. *102*, 207–226.

Hong, A., Lee-Kong, S., Iida, T., Sugimura, I., and Lilly, M.A. (2003). The p27cip/kip ortholog dacapo maintains the *Drosophila* oocyte in prophase of meiosis I. Development *130*, 1235–1242.

Hsieh, M., Lee, D., Panigone, S., Horner, K., Chen, R., Theologis, A., Lee, D.C., Threadgill, D.W., and Conti, M. (2007). Luteinizing hormone-dependent activation of the epidermal growth factor network is essential for ovulation. Mol. Cell. Biol. *27*, 1914–1924.

Hunt, P.A., and Hassold, T.J. (2008). Human female meiosis: what makes a good egg go bad? Trends Genet. *24*, 86–93.

Hutt, K.J., and Albertini, D.F. (2007). An oocentric view of folliculogenesis and embryogenesis. Reprod. Biomed. Online *14*, 758–764.

Jaffe, L.A., Norris, R.P., Freudzon, M., Ratzan, W.J., and Mehlmann, L.M. (2009). Microinjection of follicle-enclosed mouse oocytes. Methods Mol. Biol. *518*, 157–173.

Kaushal, N., and Bansal, M.P. (2007). Inhibition of CDC2/Cyclin B1 in response to selenium-induced oxidative stress during spermatogenesis: potential role of Cdc25c and p21. Mol. Cell. Biochem. *298*, 139–150.

Kitajima, T.S., Ohsugi, M., and Ellenberg, J. (2011). Complete kinetochore tracking reveals error-prone homologous chromosome biorientation in mammalian oocytes. Cell *146*, 568–581.

Kolano, A., Brunet, S., Silk, A.D., Cleveland, D.W., and Verlhac, M.H. (2012). Error-prone mammalian female meiosis from silencing the spindle assembly checkpoint without normal interkinetochore tension. Proc. Natl. Acad. Sci. USA *109*, E1858–E1867.

Kouznetsova, A., Hernández-Hernández, A., and Höög, C. (2014). Merotelic attachments allow alignment and stabilization of chromatids in meiosis II oocytes. Nat. Commun. *5*, 4409.

Kulukian, A., Han, J.S., and Cleveland, D.W. (2009). Unattached kinetochores catalyze production of an anaphase inhibitor that requires a Mad2 template to prime Cdc20 for BubR1 binding. Dev. Cell *16*, 105–117.

Lane, S.I., and Jones, K.T. (2014). Non-canonical function of spindle assembly checkpoint proteins after APC activation reduces aneuploidy in mouse oocytes. Nat. Commun. *5*, 3444.

Ledan, E., Polanski, Z., Terret, M.E., and Maro, B. (2001). Meiotic maturation of the mouse oocyte requires an equilibrium between cyclin B synthesis and degradation. Dev. Biol. *232*, 400–413.

Lefèvre, B., Pesty, A., Koziak, K., and Testart, J. (1992). Protein kinase C modulators influence meiosis kinetics but not fertilizability of mouse oocytes. J. Exp. Zool. *264*, 206–213.

LeMaire-Adkins, R., Radke, K., and Hunt, P.A. (1997). Lack of checkpoint control at the metaphase/anaphase transition: a mechanism of meiotic nondisjunction in mammalian females. J. Cell Biol. *139*, 1611–1619.

Levy-Nissenbaum, O., Sagi-Assif, O., Raanani, P., Avigdor, A., Ben-Bassat, I., and Witz, I.P. (2003). Overexpression of the dual-specificity MAPK phosphatase PYST2 in acute leukemia. Cancer Lett. *199*, 185–192.

Lincoln, A.J., Wickramasinghe, D., Stein, P., Schultz, R.M., Palko, M.E., De Miguel, M.P., Tessarollo, L., and Donovan, P.J. (2002). Cdc25b phosphatase is required for resumption of meiosis during oocyte maturation. Nat. Genet. *30*, 446–449.

Liu, D., Vleugel, M., Backer, C.B., Hori, T., Fukagawa, T., Cheeseman, I.M., and Lampson, M.A. (2010). Regulated targeting of protein phosphatase 1 to the outer kinetochore by KNL1 opposes Aurora B kinase. J. Cell Biol. *188*, 809–820.

London, N., and Biggins, S. (2014). Signalling dynamics in the spindle checkpoint response. Nat. Rev. Mol. Cell Biol. *15*, 736–747.

Lüscher, B., Brizuela, L., Beach, D., and Eisenman, R.N. (1991). A role for the p34cdc2 kinase and phosphatases in the regulation of phosphorylation and disassembly of lamin B2 during the cell cycle. EMBO J. *10*, 865–875.

Madissoon, E., Töhönen, V., Vesterlund, L., Katayama, S., Unneberg, P., Inzunza, J., Hovatta, O., and Kere, J. (2014). Differences in gene expression between mouse and human for dynamically regulated genes in early embryo. PLoS ONE *9*, e102949.

Maia, A.R., Garcia, Z., Kabeche, L., Barisic, M., Maffini, S., Macedo-Ribeiro, S., Cheeseman, I.M., Compton, D.A., Kaverina, I., and Maiato, H. (2012). Cdk1 and Plk1 mediate a CLASP2 phospho-switch that stabilizes kinetochore-microtubule attachments. J. Cell Biol. *199*, 285–301.

Marangos, P., Verschuren, E.W., Chen, R., Jackson, P.K., and Carroll, J. (2007). Prophase I arrest and progression to metaphase I in mouse oocytes are controlled by Emi1-dependent regulation of APC(Cdh1). J. Cell Biol. *176*, 65–75.

McCloy, R.A., Rogers, S., Caldon, C.E., Lorca, T., Castro, A., and Burgess, A. (2014). Partial inhibition of Cdk1 in G 2 phase overrides the SAC and decouples mitotic events. Cell Cycle *13*, 1400–1412.

Mitri, F., Bentov, Y., Behan, L.A., Esfandiari, N., and Casper, R.F. (2014). A novel compound heterozygous mutation of the luteinizing hormone receptor—implications for fertility. J. Assist. Reprod. Genet. *31*, 787–794.

Nijenhuis, W., Vallardi, G., Teixeira, A., Kops, G.J., and Saurin, A.T. (2014). Negative feedback at kinetochores underlies a responsive spindle checkpoint signal. Nat. Cell Biol. *16*, 1257–1264.

Oh, J.S., Han, S.J., and Conti, M. (2010). Wee1B, Myt1, and Cdc25 function in distinct compartments of the mouse oocyte to control meiotic resumption. J. Cell Biol. *188*, 199–207.

Okazaki, K., Hayashida, K., Iwashita, J., Harano, M., Furuno, N., and Sagata, N. (1996). Isolation of a cDNA encoding the *Xenopus* homologue of mammalian Cdc25A that can induce meiotic maturation of oocytes. Gene *178*, 111–114.

Perdiguero, E., and Nebreda, A.R. (2004). Regulation of Cdc25C activity during the meiotic G2/M transition. Cell Cycle *3*, 733–737.

Pfender, S., Kuznetsov, V., Pasternak, M., Tischer, T., Santhanam, B., and Schuh, M. (2015). Live imaging RNAi screen reveals genes essential for meiosis in mammalian oocytes. Nature *524*, 239–242.

Pirino, G., Wescott, M.P., and Donovan, P.J. (2009). Protein kinase A regulates resumption of meiosis by phosphorylation of Cdc25B in mammalian oocytes. Cell Cycle *8*, 665–670.

Pomerening, J.R., Ubersax, J.A., and Ferrell, J.E., Jr. (2008). Rapid cycling and precocious termination of G1 phase in cells expressing CDK1AF. Mol. Biol. Cell *19*, 3426–3441.

Primorac, I., and Musacchio, A. (2013). Panta rhei: the APC/C at steady state. J. Cell Biol. *201*, 177–189.

Rattani, A., Vinod, P.K., Godwin, J., Tachibana-Konwalski, K., Wolna, M., Malumbres, M., Novák, B., and Nasmyth, K. (2014). Dependency of the spindle assembly checkpoint on Cdk1 renders the anaphase transition irreversible. Curr. Biol. *24*, 630–637.

Reis, A., Chang, H.Y., Levasseur, M., and Jones, K.T. (2006). APCcdh1 activity in mouse oocytes prevents entry into the first meiotic division. Nat. Cell Biol. *8*, 539–540.

Richards, J.S., Russell, D.L., Ochsner, S., and Espey, L.L. (2002). Ovulation: new dimensions and new regulators of the inflammatory-like response. Annu. Rev. Physiol. *64*, 69–92.

Schmitt, A., and Nebreda, A.R. (2002). Signalling pathways in oocyte meiotic maturation. J. Cell Sci. *115*, 2457–2459.

Sironi, L., Melixetian, M., Faretta, M., Prosperini, E., Helin, K., and Musacchio, A. (2001). Mad2 binding to Mad1 and Cdc20, rather than oligomerization, is required for the spindle checkpoint. EMBO J. *20*, 6371–6382.

Suijkerbuijk, S.J., Vleugel, M., Teixeira, A., and Kops, G.J. (2012). Integration of kinase and phosphatase activities by BUBR1 ensures formation of stable kinetochore-microtubule attachments. Dev. Cell *23*, 745–755.

Tanoue, T., Yamamoto, T., and Nishida, E. (2002). Modular structure of a docking surface on MAPK phosphatases. J. Biol. Chem. *277*, 22942–22949.

Touati, S.A., and Wassmann, K. (2016). How oocytes try to get it right: spindle checkpoint control in meiosis. Chromosoma *125*, 321–335.

Traxler, P., Furet, P., Mett, H., Buchdunger, E., Meyer, T., and Lydon, N. (1997). Design and synthesis of novel tyrosine kinase inhibitors using a pharmacophore model of the ATP-binding site of the EGF-R. J. Pharm. Belg. *52*, 88–96.

Verlhac, M.H., Lefebvre, C., Kubiak, J.Z., Umbhauer, M., Rassinier, P., Colledge, W., and Maro, B. (2000). Mos activates MAP kinase in mouse oocytes through two opposite pathways. EMBO J. *19*, 6065–6074.

Wassmann, K., Niault, T., and Maro, B. (2003). Metaphase I arrest upon activation of the Mad2-dependent spindle checkpoint in mouse oocytes. Curr. Biol. *13*, 1596–1608.

Whalley, H.J., Porter, A.P., Diamantopoulou, Z., White, G.R., Castañeda-Saucedo, E., and Malliri, A. (2015). Cdk1 phosphorylates the Rac activator Tiam1 to activate centrosomal Pak and promote mitotic spindle formation. Nat. Commun. *6*, 7437.

Yano, K., Uesono, Y., Yoshida, S., Kikuchi, A., Kashiwazaki, J., Mabuchi, I., and Kikuchi, Y. (2013). Mih1/Cdc25 is negatively regulated by Pkc1 in *Saccharomyces cerevisiae*. Genes Cells *18*, 425–441.

Yoshida, M., Feng, W., Nishio, K., Takahashi, M., Heike, Y., Saijo, N., Wakasugi, H., and Ikekawa, T. (2001). Antitumor action of the PKC activator gnidimacrin through cdk2 inhibition. Int. J. Cancer *94*, 348–352.

Zhang, D., Li, M., Ma, W., Hou, Y., Li, Y.H., Li, S.W., Sun, Q.Y., and Wang, W.H. (2005). Localization of mitotic arrest deficient 1 (MAD1) in mouse oocytes during the first meiosis and its functions as a spindle checkpoint protein. Biol. Reprod. *72*, 58–68.

Zhang, P., Zucchelli, M., Bruce, S., Hambiliki, F., Stavreus-Evers, A., Levkov, L., Skottman, H., Kerkelä, E., Kere, J., and Hovatta, O. (2009). Transcriptome profiling of human pre-implantation development. PLoS ONE *4*, e7844.

Zielinska, A.P., Holubcova, Z., Blayney, M., Elder, K., and Schuh, M. (2015). Sister kinetochore splitting and precocious disintegration of bivalents could explain the maternal age effect. eLife *4*, e11389.

**Cell Reports, Volume *17***

## Supplemental Information

# The Phosphatase Dusp7 Drives Meiotic Resumption and Chromosome Alignment in Mouse Oocytes

**Thomas Tischer and Melina Schuh**

**Supplemental Files for**

**Title:**

# The phosphatase Dusp7 drives meiotic resumption and chromosome alignment in mouse oocytes

**Authors:** Thomas Tischer[1] and Melina Schuh[1,2]*

**Affiliations:**

[1] Medical Research Council, Laboratory of Molecular Biology, Francis Crick Avenue, Cambridge Biomedical Campus, Cambridge CB2 0QH, United Kingdom

[2] Max-Planck-Institut für biophysikalische Chemie, Am Faßberg 11, 37077 Göttingen, Germany

**Contact Information**

*Correspondence to: Melina Schuh (melina.schuh@mpibpc.mpg.de)

## Supplemental Experimental Procedures

*Vectors*

eGFP-DUSP7 as well as H2B-mRFP and eGFP-MAP4 constructs were described before (Pfender et al., 2015; Schuh and Ellenberg, 2007). Cdk1, CyclinB1, CDC25B and MAD1 were amplified from cDNA and inserted into pGEMHE vectors with the corresponding tags. cPKC constructs were obtained from I. Vallis (MRC Laboratory of Molecular Biology, Cambridge, UK) and cloned into pGEMHE for mRNA preparation. HA-MAPK in pCDNA3.1 was from Addgene (8974) (Dimitri et al., 2005). For immunoprecipitation experiments with DUSP7 the eGFP-tag in pEGFP was replaced by a Flag-tag. For bacterial expression DUSP7 was cloned via Gibson Assembly (New England Biolabs) into pET28a(+). To create point mutants the QuikChange II XL Site-Directed Mutagenesis Kit (Agilent) was used. In DUSP7, cysteine 333 was replaced with serine (C333S) to create the catalytically inactive mutant. In the MAPK binding mutant arginine 104 and 105 were replaced by methionine (R104/105M). Similarly, threonine 14 and tyrosine 15 in Cdk1 were replaced by alanine and phenylalanine, respectively, to obtain $Cdk1^{AF}$.

*Immunoprecipitation of Flag-DUSP7 and HA-MAPK from HeLa cells*

HeLa cells were plated on 10 cm plates and transfected using Fugene 6 (Promega) according to manufacturer's instructions. Expression was performed for 48h and cells were removed from the plates by trypsin. Subsequently, they were washed two times with PBS and resuspended in lysis buffer (Tanoue et al., 2002). Immunoprecipitation with M2-Flag-agarose (Sigma) was performed as described by the manufacturer,

except that lysis buffer was used for washing. Input and immunoprecipitated samples were analyzed by SDS PAGE and immunoblotting.

*Quantitative RT-PCR*

Total RNA was isolated from at least ten oocytes with the RNeasy Mirco Plus Kit (Qiagen) and subsequently used for a reverse transcription PCR with the High Capacity RNA to cDNA Kit (Applied Biosystems). Quantitative real time PCR was performed with the SYBR green master mix (Applied Biosystems) on a ViiA 7 Real-Time PCR System (Applied Biosystems) according to the manufactures instructions. The oligo pairs used for GAPDH were 5'-AGAGCTGAACGGGAAGCTCACT-3' and 5'-TGCCTGCTTCACCACCTTCTTGAT-3', for DUSP7 5'-TCACCTACAAGCAAATCCCC-3' and 5'-TGTCACTGAACGGCTGATG-3', and for PKCβ 5'-TTAACTTCCTGATGGTGCTGG-3' and 5'-GAGTTCATCTGTACCCTTCCG-3'.

*Purification of His-DUSP7 from Bacteria*

His-tagged DUSP7 was expressed in *E.coli* strain BL21(DE3) overnight at 18 °C. Bacteria were pelleted the next morning and washed once with PBS. They were taken up in IMAC 5 buffer (20 mM Tris pH 8, 300 mM NaCl, 5 mM Imidazole, complete protease inhibitors (Roche)) and lysed using an EmulsiFlex C5. After centrifugation for 20 minutes at 25.000 g the supernatant was added on Ni-IDA agarose (Macherey and Nagel) and incubated for at least 3 h at 4 °C to allow binding. Subsequently, the beads were washed once in IMAC 20 buffer (see IMAC 5, but 20 mM Imidazole instead), once in IMAC 80 buffer + 1 mM MgATP + 0.1% Triton X-100, twice in

IMAC 80 buffer. Elution was performed on a small column with one bead volume of IMAC 500 buffer.

The purity of the purified protein was analyzed by SDS PAGE and Instant Blue (Expedeon) staining. The activity was determined by a para-Nitrophenyl Phosphate (pNPP, New England Biolabs) assay (Dowd et al., 1998).

*In vitro phospho-peptide screening assay and generation of the Venn diagram*

Screening plates containing the synthesized peptides were purchased from JPT (product codes PhSS-Y-360-250 and PhSS-360-250). The same assay buffer as for the pNPP assay was used for the screening and the assay was incubated for 2 h at 37 °C. The reaction was stopped with Biomol green solution (Enzo) and incubated for 15 min at room temperature to allow color development. A Tecan F200 plate reader was used to analyze the absorbance at 620 nm. For each assay, Z*-scores were calculated individually and a value greater than two was considered significant (Zhang, 2011). All potential hits were used as input to create a Venn diagram with help of the website http://www.interactivenn.net/ (Heberle et al., 2015). The list of hits including all reads and the Z*-scores is available as Supplemental File S5. The interactive Venn diagram can be recreated using Supplemental File S6 as input on the above mentioned website.

*Histone H1 kinase assay*

All oocytes where inspected using a dissection stereo microscope every 30 minutes. The first oocytes that performed NEBD were grouped together and left aside. They were taken as the last sample (6h post NEBD). The same procedure was performed

for the 5h time point. This ensures that only oocytes that underwent NEBD were used for the later time points. These are also the time points which were analyzed for Cdk1 kinase activity in Figure 3 B. We used the same procedure for all Cdk1 kinase assays that are shown in the manuscript. Three mouse oocytes in the desired stage of development were transferred into a reaction tube and snap frozen in liquid nitrogen. To thaw them, 2.5 µL of two-fold concentrated H1 oocyte lysis buffer (160 mM beta-glycero-phosphate, 40 mM EGTA, 30 mM $MgCl_2$, 2 mM DTT, 2x EDTA-free complete protease inhibitors (Roche)) was added and the oocytes were lysed by vortexing and centrifugation at 20.000 rpm, 4 °C. By addition of 2.5 µL two-fold concentrated H1 solution (2 mg/mL purified Histon H1 (Millipore), 0.5 mCi/mL gamma-$^{33}$P-ATP) the reactions were started and incubated at 30 °C for 30 min. The reactions were stopped by adding 5 µL two-fold concentrated laemmli sample buffer and heated at 95 °C for 5 min. Samples were separated via SDS-PAGE and the gel was stained with Instant Blue (Expedeon). After drying on a sheet of Whatman paper, incorporation of $^{33}$P was analyzed by autoradiography.

**Supplemental References**

Dimitri, C.A., Dowdle, W., MacKeigan, J.P., Blenis, J., and Murphy, L.O. (2005). Spatially separate docking sites on ERK2 regulate distinct signaling events in vivo. Curr. Biol. 15, 1319–1324.

Dowd, S., Sneddon, A.A., and Keyse, S.M. (1998). Isolation of the human genes encoding the pyst1 and Pyst2 phosphatases: characterisation of Pyst2 as a cytosolic dual-specificity MAP kinase phosphatase and its catalytic activation by both MAP and SAP kinases. J. Cell Sci. 111, 3389–3399.

Heberle, H., Meirelles, G.V., da Silva, F.R., Telles, G.P., and Minghim, R. (2015). InteractiVenn: a web-based tool for the analysis of sets through Venn diagrams. BMC Bioinformatics 16, 169.

Schuh, M., and Ellenberg, J. (2007). Self-organization of MTOCs replaces centrosome function during acentrosomal spindle assembly in live mouse oocytes. Cell 130, 484–498.

Zhang, X.D. (2011). Illustration of SSMD, z score, SSMD*, z* score, and t statistic for hit selection in RNAi high-throughput screens. J. Biomol. Screen. 16, 775–785.

**Supplemental Figures S1 – S4** (including figure legends): All Supplemental Figures refer directly to the main Figures with the same number (e.g. Supplemental Fig. S1 is related Fig. 1).

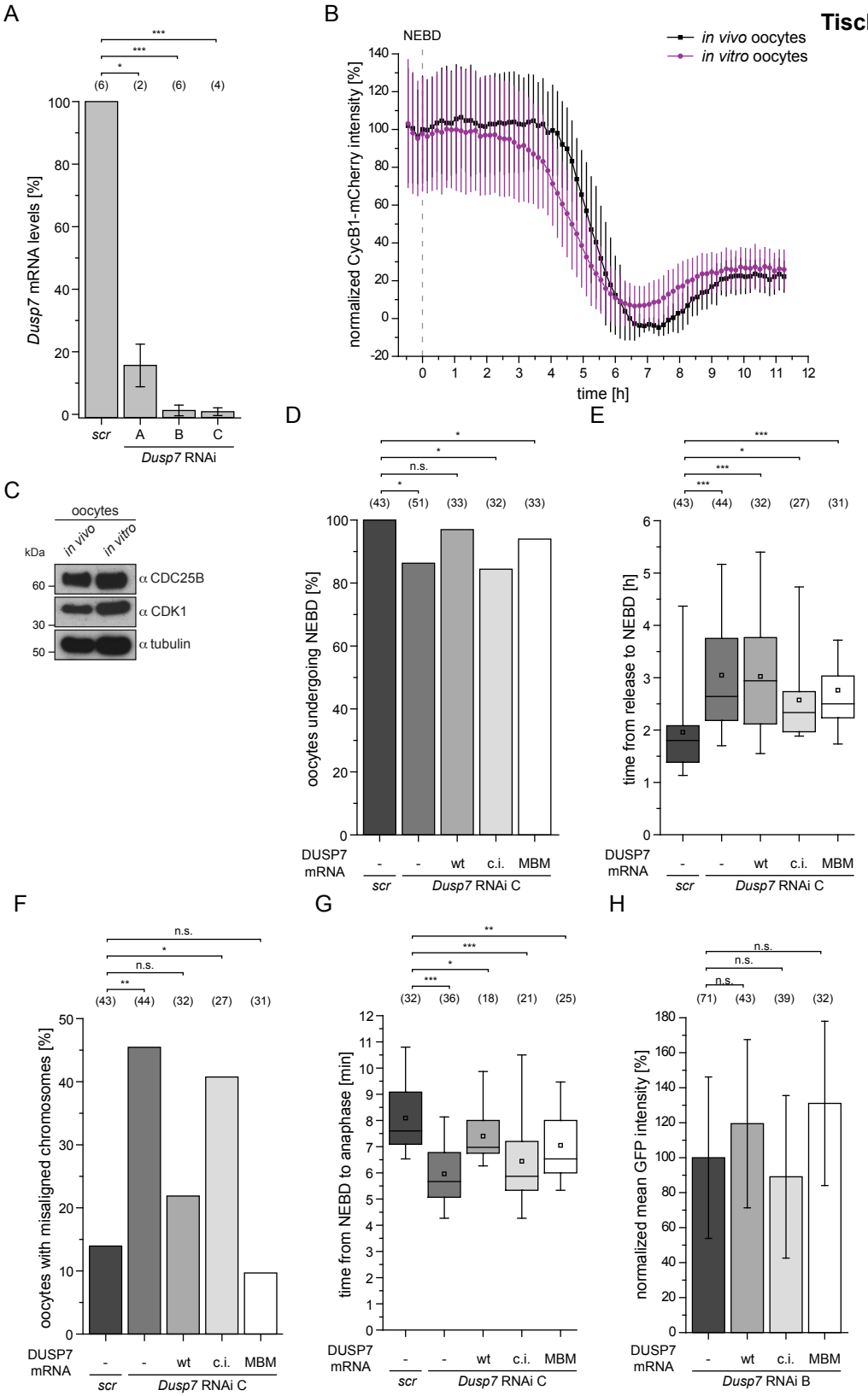


**Supplementary Figure S1 (Related to Figure 1)**

(A) Quantitative real time PCR to analyze the levels of *Dusp7* mRNA after DUSP7 depletion. Due to the lack of suitable antibodies, we were unable to directly asses our depletion efficiency of DUSP7 by immunoblotting. Therefore we evaluated the depletion based on the remaining *Dusp7*-mRNA levels by quantitative real time PCR. Out of the three tested siRNA-oligos we had two that very efficiently depleted DUSP7 and showed a comparable phenotype (Fig. 1 and S1). For all further experiments we used oligo “B”. To ensure specificity and reproducablity we repeated all experiments shown in Fig. 1 also with oligo “C” (see D - G). We did not observe any differences in the behavior of both siRNA oligos. The experiment was repeated three times.

(B) Follicles were isolated and cultured for 10 days *in vitro*. Oocytes from mature mice from the same strain as the follicles were isolated at the day of the experiment (*in vivo*). *In vitro* and *in vivo* grown oocytes were injected with H2B-mCherry to mark the chromosomes and Cyclin B1-mCherry. After expression, all oocytes were released from prophase arrest and imaged under a convocal microscope. The Cyclin B1-mCherry fluorescence was measured as described in (Lane and Jones, 2014). The average fluorescence intensity at NEBD was set to 100%. The CycB1 degradation dynamics of *in vivo* and *in vitro* grown oocytes are similar. The experiment was repeated three times.

(C) Immunoblot of *in vivo* and *in vitro* grown oocytes. Oocytes were isolated as described in (B) but not injected. Oocytes were lysed in laemmli sample buffer. Proteins were separated by SDS PAGE and immunoblotted for the indicated cell cycle proteins. 30 *in vivo* grown and 40 *in vitro* grown oocytes were loaded. All tested proteins are present at similar levels in *in vivo* and *in vitro* grown oocytes.

(D) Follicles were isolated and microinjected with scrambled (*scr*) or *Dusp7* RNAi oligo C. After ten days of culture the surrounding somatic cells were removed and the mature oocytes were injected again with H2B-mCherry to label the chromosomes and eGFP-MAP4 to label the meiotic spindle and analyzed for NEBD. The rescue constructs were wildtype DUSP7 (wt), catalytically inactive DUSP7 (c.i.), and MAPK binding mutant DUSP7 (MBM). GFP expression denotes expression of no DUSP7 rescue construct. The experiment was repeated five times.

(E) Oocytes from (D) were analyzed for the time from release from prophase arrest to NEBD.

(F) Oocytes from (D) that underwent NEBD were analyzed for the presence of misaligned chromosomes in the frame before the onset of anaphase.

(G) The same oocytes as in (D) were used. The time in hours that the oocytes needed from NEBD to anaphase was analyzed.

(H) The mean intensity of the GFP signal from the oocytes used in Fig. 1 B was measured. All intensities were normalized to the corresponding GFP-only expressing oocytes (-) from the same experiment. The mean from all oocytes +/- s.d. is shown.

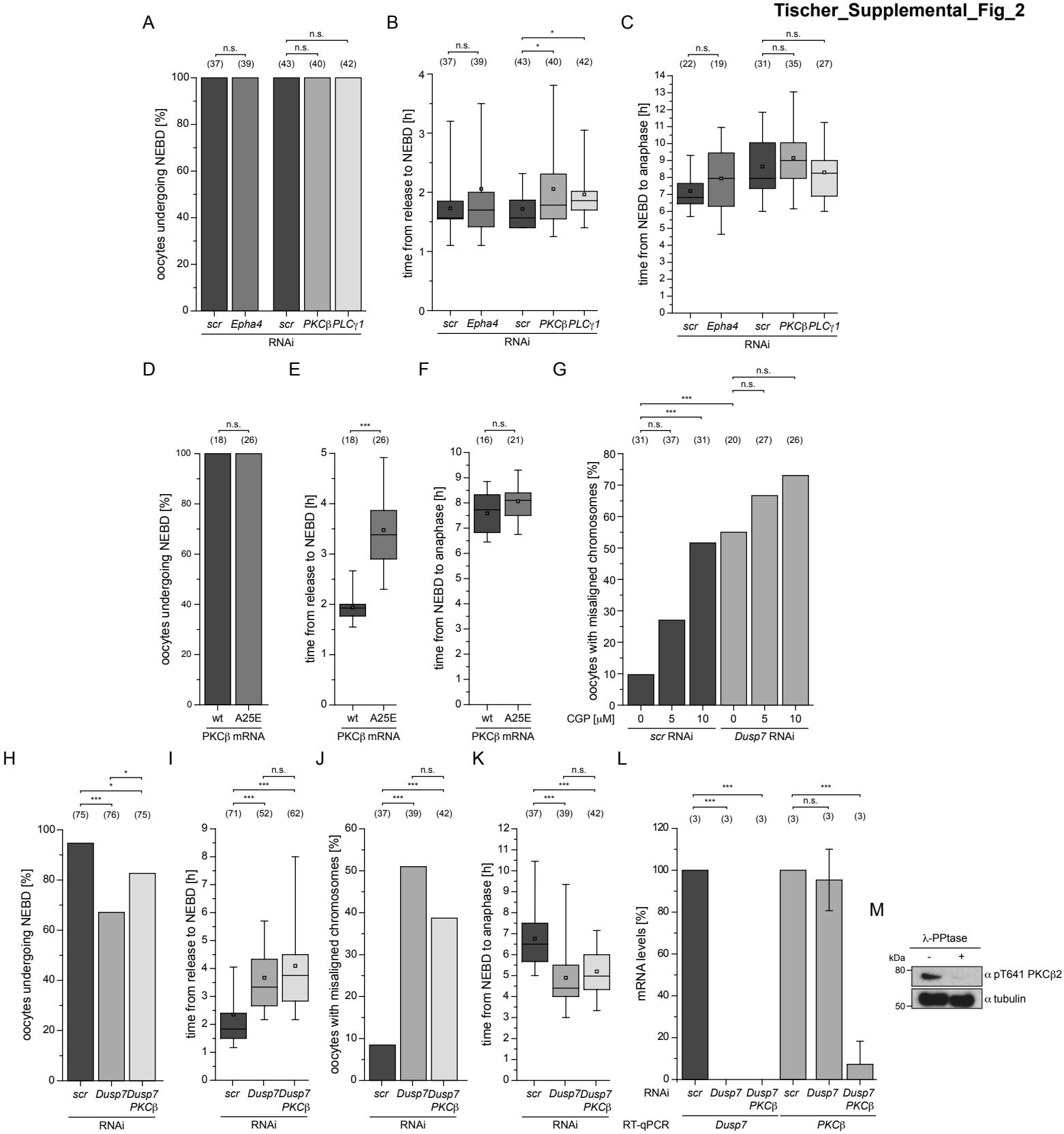


**Supplementary Figure S2 (Related to Figure 2)**

(A) Follicles were isolated and microinjected with scrambled (*scr*), *Epha4*, *PKCβ*, or *PLCγ1* RNAi. After ten days of culture the surrounding somatic cells were removed and the mature oocytes were microinjected again with H2B-mCherry to label the chromosomes and eGFP-MAP4 to label the meiotic spindle. The oocytes were imaged on a confocal microscope and analyzed for NEBD at the end of the imaging. The experiment was repeated three times.

(B) Oocytes from (A) were analyzed for the time from release from prophase arrest until the oocytes underwent NEBD.

(C) The same oocytes as in (A) were used. The time that the oocytes needed from NEBD to anaphase onset was analyzed.

(D) Mature oocytes were microinjected with H2B-mCherry and GFP-PKCβ$^{wt}$ or GFP-PKCβ$^{A25E}$. After mRNA expression the oocytes were released from prophase arrest, imaged on a confocal microscope and analyzed for NEBD at the end of the imaging.The experiment was repeated three times.

(E) The oocytes from (D) were analyzed for their time from release from prophase arrest until the oocytes underwent NEBD. We believe that simultaneous activation of several cPKC isoforms in PMA treated oocytes results in a much stronger defect compared to over-expression of only one active isoform.

(F) Oocytes from (D) were analyzed for the time they spend from NEBD to anaphase onset.

(G) Oocytes from Fig. 2 E were analyzed for the presence of misaligned chromosomes in the frame before anaphase onset. We were reluctant to use even higher concentrations of the inhibitor since we observed an increase in misaligned chromosomes already in control oocytes.

(H) Follicles were isolated and microinjected with scrambled (*scr*), *Dusp7*, and *Dusp7* + *PKCβ* RNAi. After the culture the mature oocytes were microinjected again with H2B-mCherry to label the chromosomes and eGFP-MAP4 to label the meiotic spindle. The oocytes were imaged on a confocal microscope and analyzed for NEBD. The experiment was repeated six times.

(I) Oocytes from (H) were analyzed for the time they needed from release from prophase arrest to NEBD.

(J) Oocytes from (H) that performed NEBD were analyzed for misaligned chromosomes in the frame before anaphase onset.

(K) Oocytes from (H) were analyzed for the time they spend from NEBD to anaphase onset.

(L) Quantitative real time PCR to analyze the levels of *Dusp7* and *PKCβ* mRNA after DUSP7 depletion or co-depletion of DUSP7 and PKCβ.

(M) Immunoblot showing the phospho-specificity of the pT641 PKCβ2 antibody. Oocytes were lysed in PMP buffer (NEB) containing 1mM $MnCl_2$ and complete protease inhibitors and were either treated for 1h at 30 °C with 100U lambda phosphatase (λ-PPtase) or BSA. 30 oocytes per lane were used.

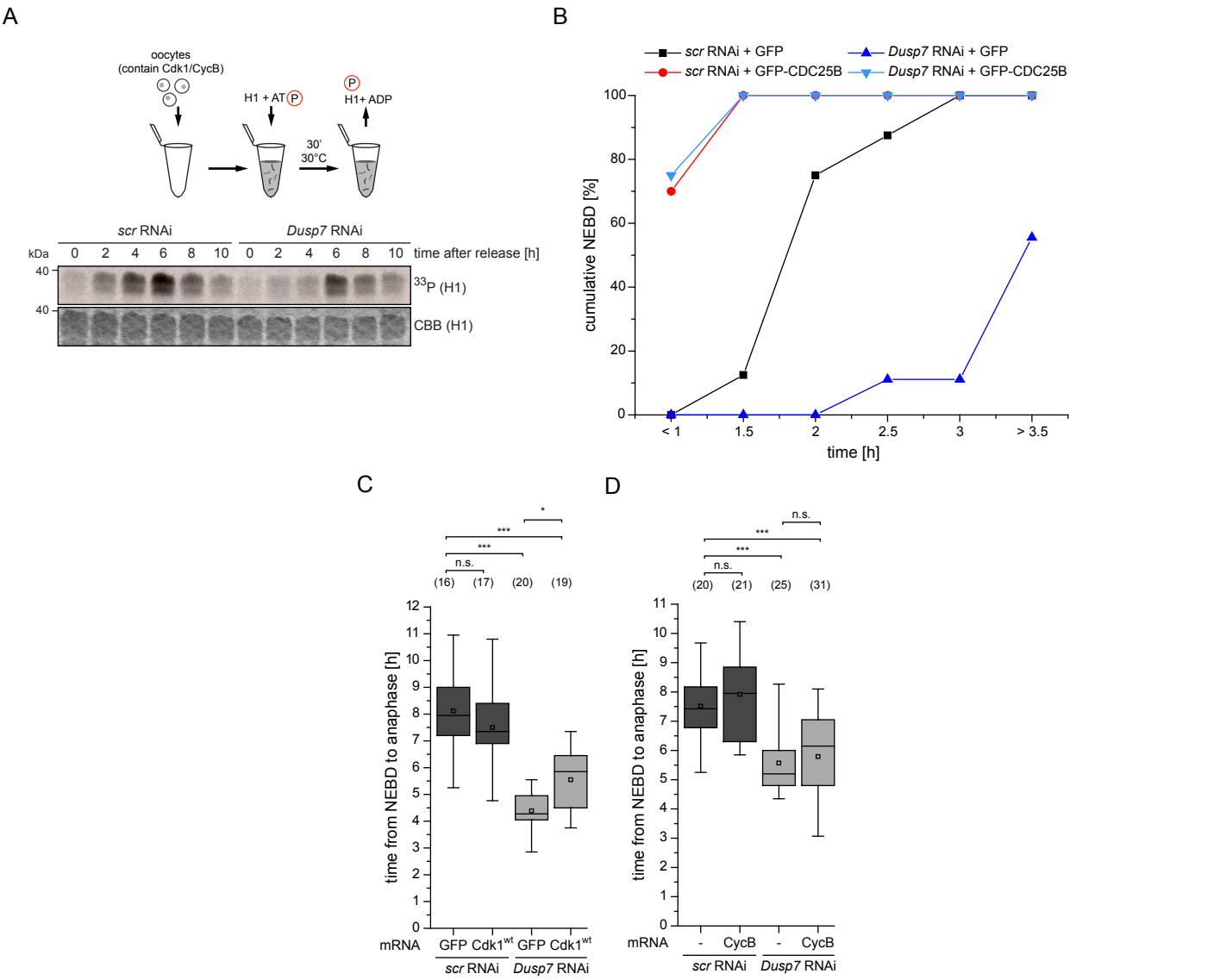


**Supplementary Figure S3 (Related to Figure 3)**
(A) Scheme showing the *in vitro* Cdk1/CycB kinase assay. Follicles were microinjected with scrambled (*scr*) or *Dusp7* RNAi. After 10 days of culture the oocytes were released and snap frozen at the indicated time points. The autoradiogram shows the incorporation of radioactive phosphate into Histone H1. Coomassie Brilliant Blue (CBB) staining shows the equal loading of Histone H1.
(B) Follicles were microinjected with scrambled (*scr*) or *Dusp7* RNAi. After the culture the oocytes were isolated and microinjected again with H2B-mCherry and GFP or GFP-CDC25B. Oocytes expressing CDC25B performed NEBD already before imaging at the microscope was started and analysis of the timing was therefore not possible. Instead, all oocytes that performed NEBD within a time frame of 60 minutes after release (and within 30 minute intervals afterwards) were grouped together. The cumulative percentage of oocytes that performed NEBD after the indicated time is shown. The experiment was repeated two times.
(C) Oocytes from Fig. 3 E were analyzed for the time they spend from NEBD to anaphase onset.
(D) Oocytes from Fig. 3 I were analyzed for the time they spend from NEBD to anaphase onset.

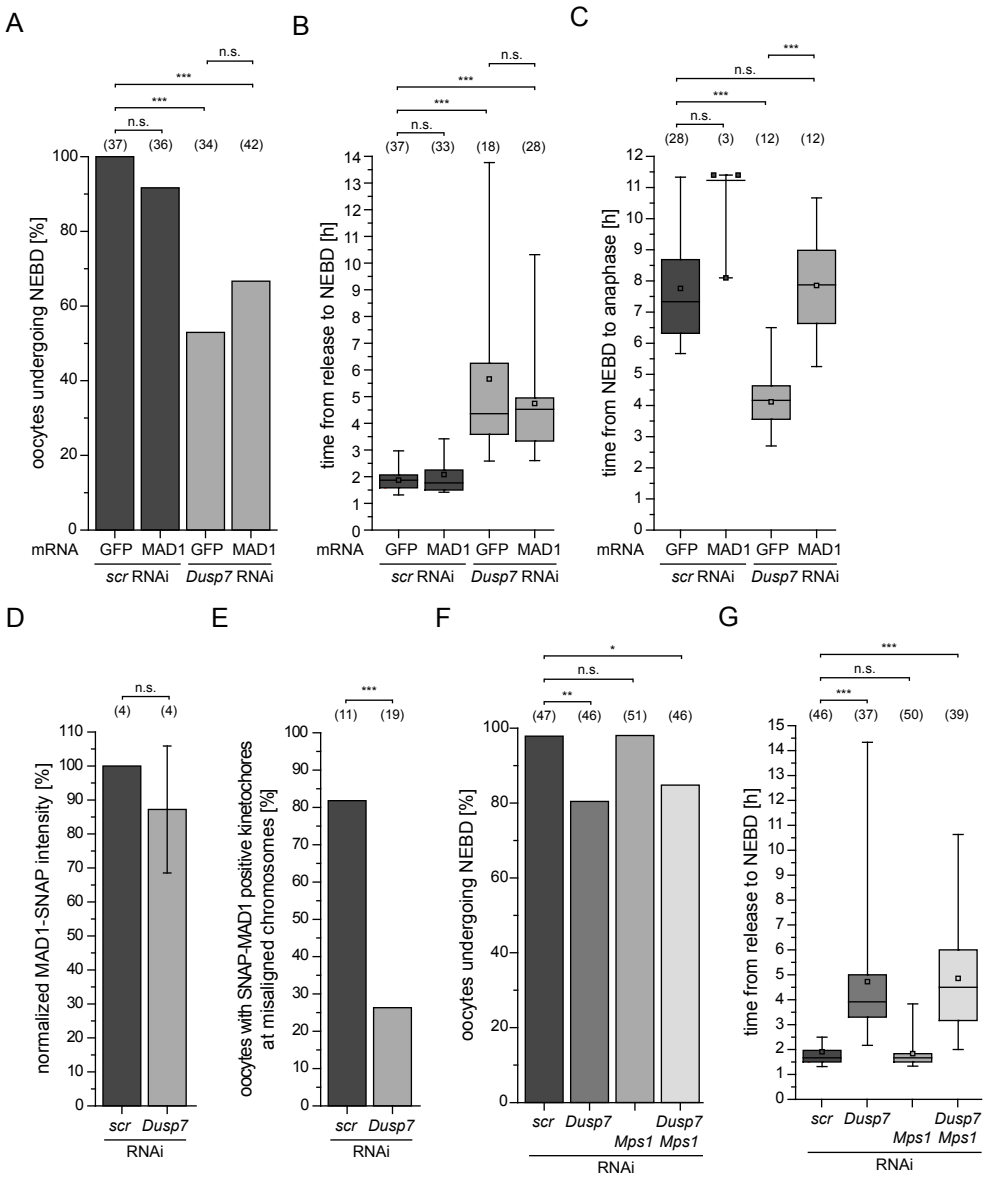


**Supplementary Figure S4 (Related to Figure 4)**

(A) Oocytes from Fig. 4 B were analyzed for the presence of NEBD at the end of the imaging.

(B) Oocytes from Fig. 4 B were analyzed for the time from release from prophase arrest to NEBD.

(C) Oocytes from Fig. 4 B that underwent NEBD were analyzed for the time from NEBD to anaphase onset. Note that for *scr*-RNAi + MAD1 expression only three oocytes underwent anaphase, because MAD1 over-expression arrests oocytes in metaphase. For this reason we opted to show the three single data points instead of the normal box plot.

(D) In oocytes from Fig. 4 A and B MAD1-SNAP intensity was measured in an area around the chromosomes 60 min after NEBD and corrected for background signal. To signal intensity was normalized for all individual experiments against *scrambled* (*scr*) RNAi injected oocytes. The mean normalized intensity of all experiments was calculated and is shown as mean +/- s.d.. MAD1-SNAP expression levels are not significantly different between *scrambled* (*scr*) and *Dusp7* RNAi treated oocytes. n is the number of experiments.

(E) Oocytes from Fig 4 A and B were analyzed for the presence of SNAP-MAD1 on transiently misaligned chromosomes upon formation of the metaphase plate.

(F) Oocytes from Fig. 4 C were analyzed for the presence of NEBD at the end of the imaging.

(G) Oocytes from Fig. 4 C were analyzed for the time from release from prophase arrest to NEBD.

**Supplemental Table S5 (Related to Figure 2)**: **Hits from the *in vitro* peptide screen**

Microsoft Excel file containing all hits from the *in vitro* phospho-peptide screens.

**Supplemental File S6 (Related to Figure 2)**: **Input data for the Venn diagram**

Input file for the website http://www.interactivenn.net/ to re-create an interactive Venn diagram with the hits from the *in vitro* phospho-peptide screen.

**Supplemental Movie S1 (Related to Figure 1)**: Full movie from the exemplary images in Fig. 1 A (top row). DNA is labeled with H2B-mCherry and shown in magenta. Microtubules are labeled with MAP4-eGFP and shown in green. The oocyte also expresses free eGFP, shown in green.

**Supplemental Movie S2 (Related to Figure 1)**: Full movie from the exemplary images in Fig. 1 A (middle row). DNA is labeled with H2B-mCherry and shown in magenta. Microtubules are labeled with MAP4-eGFP and shown in green. The oocyte also expresses free eGFP, shown in green.

**Supplemental Movie S3 (Related to Figure 1)**: Full movie from the exemplary images in Fig. 1 A (bottom row). DNA is labeled with H2B-mCherry and shown in magenta. Microtubules are labeled with MAP4-eGFP and shown in green. The oocyte also expresses free eGFP, shown in green.

**Supplemental Movie S4 (Related to Figure 4)**: Full movie from the exemplary images in Fig. 4 A (top row). DNA is labeled with H2B-mCherry and shown in magenta. MAD1-SNAP was labeled with SNAP-Cell 505 Star (New England Biolabs) and is shown in green.

**Supplemental Movie S5 (Related to Figure 4)**: Full movie from the exemplary images in Fig. 4 A (bottom row). DNA is labeled with H2B-mCherry and shown in magenta. MAD1-SNAP was labeled with SNAP-Cell 505 Star (New England Biolabs) and is shown in green.